PRNC-164

PUERTO RICO NUCLEAR CENTER

GAS STOPPING POWER MEASUREMENTS FOR ALPHA PARTICLES

Eddie Ortiz and Gilberto M. Arenas Rosillo

May 1973

OPERATED BY UNIVERSITY OF PUERTO RICO UNDER CONTRACT
NO. AT (40-1)-1833 FOR U S ATOMIC ENERGY COMMISSION

University of Puerto Rico
Mayaguez Campus

GAS STOPPING POWER MEASUREMENTS FOR ALPHA PARTICLES

by

Gilberto M. Arenas Rosillo

A thesis submitted in partial fulfillment
of the requirements for the degree of

Master of Science

(Nuclear Engineering)

May 1973

Approved:

Chairman Graduate Committee — May 7, 1973 — Date

Acting Director of Department — May 7, 1973 — Date

Director, Graduate Studies — Date

ABSTRACT

A method has been developed to measure the stopping powers of gases for alpha particles using a (Si) semiconductor detector mounted opposite a natural Am^{241} alpha source in a gas chamber and a 1024-channel data acquisition system.

By varying the gas pressure and taking an energy loss measurement at each pressure, the stopping powers and molecular stopping cross sections were calculated; also, range-energy relationships were measured simultaneously.

Experimental data are given for air, N_2, O_2, CO_2, N_2O, A, Kr, Freon 14, CH_4, C_2H_4, C_2H_6, C_3H_6 and C_3H_8 for alpha particle in the range 0.3-5.0 MeV alpha energy. The estimated probable error in the cross sections ranges from approximately 4-5 per cent at the highest energies to approximately 9-10 per cent at the lowest energies.

ACKNOWLEDGEMENT

It is the author's wish to express his sincere gratitude to those who helped him to complete this project:

To DR. EDDIE ORTIZ, Senior Scientist, Nuclear Engineering Division, Puerto Rico Nuclear Center, for suggesting the problem, for his dedicated guidance and competent supervision of the work.

To DR. AVIVA E. GILEADI, Professor, Nuclear Engineering Department, UPR-RUM, for her constructive criticism and for her valuable advice.

To DR. DONALD S. SASSCER, Head of the Nuclear Engineering Department, UPR-RUM, for his sincere interest in the author's work.

To the Colombian Ministry of Mines and Petroleum-ICETEX Foundation for granting the financial assistance needed for completion of this project.

To the personnel of the Library and Reproduction office of the PRNC for their exemplary cooperation.

DEDICATION

To my dear Esther

and Alejandro

TABLE OF CONTENTS

LIST OF TABLES

LIST OF TABLES CONT.

LIST OF FIGURES

LIST OF FIGURES CONT.

Figure No. Page

CHAPTER I

INTRODUCTION

In recent years there has been a considerable interest in data relating to stopping power of charged particles in various materials. The significance of this parameter may be particulary appreciated by elementary-particle physicists and nuclear physicists in view of the fact that the precision with which nuclear reaction cross sections can be measured often depends on the accuracy with which the stopping cross section of the target material is known. Health physicists need stopping power measurements for radiation protection purposes because biological, chemical and physical effects produced by the charged particle deposition in a medium like human soft tissue (of composition: H 10.1%, C 12.1%, N 4% and O 73.6% by weight) depends among other things, on the absorbed dose and on the linear energy transfer of the charged particle involved.

Energy deposition in the material through which the radiation is passing (stopping material), is closely related to the energy loss by the penetrating radiation. The energy loss of the penetrating charged particle per unith path length in the stopping material is called the stopping power of the material. Stopping power is dependent upon the various mechanisms in which radiation interacts with individual atoms and molecules and is an expression of the average outcome of a large number of individual interactions.

Stopping power measurements have been carried out in various solids, liquid and gases as stopping materials. In this work, a method is developed for measuring the stopping power of several organic and inorganic gases for alpha particles as a function of energy, using a semiconductor detector. By varying the gas pressure and taking an energy loss measurement at each pressure, stopping power curves and molecular stopping cross sections as a function of alpha energy have been calculated. Also, range curves and range-energy relationship for 0.3 - 5.4 MeV alpha particles in air and hydrocarbon gases were developed simultaneously. Results agreed within a 5 - 10% of accuracy with respect to literature related data.

CHAPTER II

REVIEW OF LITERATURE

As indicated by recent professional literature, there is a renewed interest in the variation of stopping power of gases for heavy charged particles (with a mass very much greater than the mass of the electron).

A large amount of experimental work has been done and theoretical expressions for stopping power have been developed showing various degrees of accuracy.

R.B.J. PALMER (11) obtained Linear Energy Transfer (dE/dx) curves for 1 to 8 Mev alpha particles in hydrocarbon gases and hydrogen.

E. ROTONDI (13) measured stopping powers for 0.1 to 5.3 alpha particles in N_2, O_2, CH_4, and CO_2 by differentiating the range-energy curves of these gases obtained by means of a variable-pressure gas cell in which Po^{210} alpha particles lose part of their energy and were detected by a semiconductor detector. These dE/dx measurements have quoted accuracies of 8 per cent between 0.1 and 0.5 Mev, 5 per cent at 1 Mev and 3 per cent at higher energies.

P.D. BOURLAND, W.K. CHU and D. POWERS (4) measured stopping cross sections for alpha particles in a differentially pumped gas-cell system from 300 Kev to 2 Mev in H_2, N_2, O_2, NH_3, N_2O, CO, CO_2, CH_4, C_2H_2, C_2H_4, C_2H_6, C_3H_6 and $(CH_2)_3$.

G.D. KERR, L.M. HAIRR, N. UNDERWOOD and A.W. WALTNER (8) reported experimental data for air, N_2, A, Kr, CO_2 and CH_4 for alpha particles in the energy range 300 Kev - 5 Mev. Molecular cross sections of the above gases were calculated within an accuracy of approximately 4 per cent of probable error at the highest energies to approximately 12 per cent at the lowest energies.

P.J. WALAH (15) measured molecular stopping cross sections for C_2H_4, C_2H_2 and C_3H_8 for 0.3 to 5 Mev alpha particles within a 10 per cent of accuracy at the lowest energies, using a variable-pressure gas cell and a constant separation distance between the alpha source and detector.

W.P. JESSE and J. SADAUSKIS (7) determined range-energy curves in the region 0 - 5 Mev for alpha particles with a collimating absorption cell and an ionization chamber. The ionization charge from a single alpha particle was collected in the ion chamber and amplified by means of the vibrating-reed electrometer.

H.A. BETHE (3) reported range-energy relations for 0 to 8 Mev alpha particles and developed a theoretical treatment on stopping power for heavy charged particles (See Section 3.3).

CHAPTER III

THE INTERACTION OF ALPHA RADIATION WITH MATTER

All radiation measurements depend on the interaction of the radiation with matter. The nature of these interactions therefore, forms the basis of a discussion of the measurements themselves, and an outline of the principal interactions of charged particles like alphas is developed in this section.

The primary mechanism of energy loss in penetrating charged particles is due to Coulomb interactions between atomic nuclei and electrons with the charged particles; to a lesser extent elastic and inelastic collisions with electrons and nuclei are also of significance. If the energy transferred to an electron is only enough to raise it to a higher level in the atom, the process is called excitation; if the electron is given enough energy to separate it completely from the atom, the process is called ionization. The two processes are closely associated and together they constitute "energy loss by collision". At energies several times the rest energy of the moving charged particle excitation and ionization account for the major part of the energy loss in all materials. Some of the electrons ejected in ionization processes have enough energies to produce further ionization themselves; such electrons are called δ-Rays.

A number of other phenomena occur when alpha particles traverse matter. Interactions with the coulomb fields of atoms, and particularly of atomic nuclei, result in change in the direction of motion of the heavy particle (the term "heavy particle" shall afterhere refer to a particle of a mass greater than that of the electron). Inelastic collisions with electrons are by far the most important processes by which a penetrating heavy charged particle loses its kinetic energy when the velocity of the particle, v, is much greater than v_o, the velocity of the electron (in hydrogen $v_o = 2.188 \times 10^8$ cm/sec, while for a 5.477-MeV alpha, $v = 1.623 \times 10^9$ cm/sec). If kinetic energy is conserved, the process is called elastic scattering; such scattering is of minor importance for heavy particles but of great importance for electrons. Scattering through a large angle entails a large acceleration of the charged particle. This in turn may result in the emission of a quantum of electromagnetic radiation, known as bremsstrahlung, which becomes important when electrons are involved.

3.1 Collision Loss and Stopping Power.- According to the classical point of view, a moving charged particle loses energy to an electron by imparting to it an impulse proportional to the strength of the coulomb force and to the time during which this force acts. Since the momentum acquired by the electron is proportional to the time during which the interaction takes place, it is inversely proportional to the velocity v, of the moving particle. The energy acquired by the electron, and hence the energy lost by the particle, must therefore, be proportional to $1/v^2$. Thus on the classical picture the energy loss per unit path length (specific energy loss) should be proportional to the electron density in the medium and inversely proportional to the square of the velocity of the particle. When the penetrating particle is moving so slowly ($v < v_0$) that is, average net charge approaches zero, the average energy loss per unit length of path to electrons decreases to zero, proportional to the velocity of the penetrating particle while the average energy loss due to elastic nuclear collisions is increasing proportional to $1/v^2$.

The charged particles moving through matter transfer their energy preferentially to those electrons that are closer to their tracks. The farther an electron is from the track of the alpha particle, the smaller the impulse it can receive, and hence the smaller the energy that can be transferred to it. If that energy is just less than the amount required to raise a K-electron to a higher energy level, no energy will be lost to a K-electron at that distance. Somewhat farther away losses to L-electron will become impossible, and so on. The more tightly bound the atomic electrons (i.e., the higher the atomic number), the shorter will be these "cut-off" distances and the smaller the rate of energy loss. Consequently the rate of energy loss is expected to show some dependence on atomic number, being smaller at high atomic numbers.

At velocities approaching the velocity of light, the $1/v^2$ dependence is modified by a relativistic effect. The relativistic contraction of the electric field of the moving alpha particle makes possible energy losses at greater distances, and in consequence the rate of energy loss increases slowly at very high energies.

The stopping power is defined as the energy lost by the heavy charged particle (alpha, in our case) per unit path in the stopping substance and is given by the expression:

$$S(E) = - (dE/dx) \tag{3.1}$$

where E is the classical kinetic energy of the particle.

Stopping power varies with the energy of the particle and the range of the particle can be calculated by:

$$R = \int_0^R dx = \int_0^{E_0} \frac{dE}{S(E)} = \int_0^{E_0} \frac{dE}{-dE/dx} \tag{3.2}$$

where R is the range and E_0 is the initial kinetic energy of the particle.

Stopping power can be determined experimentally by measuring the energy of the particles, which have gone through a certain thickness os substance. If the rango is known as a function of E, the stopping power can be obtained from:

$$\frac{dR}{dE} = \frac{1}{S(E)} \tag{3.3}$$

3.2 Stopping Cross Section.- The molecular stopping cross section ε is defined as the energy loss per molecule per unit area normal to the path of the particle, i.e.:

$$\varepsilon = -\frac{1}{n}\frac{\Delta E}{\Delta x} = -\frac{1}{n}\frac{(E_2 - E_1)}{\Delta x} \tag{3.4}$$

where $\Delta E/\Delta x$ is the energy loss per unit path length or linear stopping power and n is the number of molecules per unit volume. The stopping cross section is used since it is a quantity independent of gas pressure or temperature.

If the distance traveled by the particle is held constant and the number of atoms along the path of the particle becomes the variable on which the energy loss depends, the above equation should be written in this form:

$$\varepsilon = -\frac{1}{d}\frac{\Delta E}{\Delta n} = -\frac{1}{d}\frac{(E_2 - E_1)}{\Delta n} \tag{3.5}$$

In both equations, E_1 represents the energy of the incident particle on the material and E_2 represents the reduced energy after penetrating $n\,\Delta x$ or $d\,\Delta n$ molecules per unit area normal to the path of the particle.

An expression can be derived for Δn in terms of the variables measured in this investigation by the use of the laws of Avogadro, Boyle and Charles with the following relationship:

$$n = \frac{\rho A}{W} \tag{3.6}$$

where ρ is the density of the stopping material, W is the atomic weight and A is the Avogadro's number. Also, we can deduct from the atomic theory:

$$n_e = n.Z \tag{3.7}$$

where n_e is the electronic density and Z is the atomic number of the substance. From Eq. (3.2) we follow:

$$R = f\,(1/n) = f\,(1/n_e) \tag{3.8}$$

But n_e is directly proportional to the density of the material ρ, so the range R will be proportional $1/\rho$. From the general law of gases,

$$P.V = \frac{M}{W} R_g.T \tag{3.9}$$

where M is the molecular mass, R_g is the gas constant, P is the pressure and T is the temperature in the volume V. Rearranging the last expression we get:

$$P = \frac{M}{V}\frac{R_gT}{W} = \rho\,\frac{R_gT}{W} \tag{3.10}$$

From Eq. (3.10) we can see that (P/T) is directly proportional to n or n_e, or inversely proportional to the range R. Written in the other way,

$$\frac{P}{T} \propto \rho \propto n \propto \frac{1}{R} \tag{3.11}$$

or,

$$\frac{P_0}{T_0 \cdot n_0} = \frac{\Delta P}{T \cdot \Delta n} \tag{3.12}$$

Rearranging the last expression,

$$\Delta n = \frac{T_o}{T} \frac{\Delta P}{P_o} n_o \tag{3.13}$$

where the subscripts "o" means standard conditions and

$$n_o = \rho_o \frac{A}{W} \tag{3.13a}$$

Inserting Eq. (3.13) into Eq. (3.5) the molecular stopping cross section can be calculated from the collected experimental data using the resultant formula:

$$\varepsilon = -\frac{W}{A} \frac{T}{T_o} \frac{P_o}{\Delta P} \frac{E_2 - E_1}{\rho_o \cdot d} \tag{3.14}$$

where the mean residual energy of the alpha particle after traversing the distance d with a pressure P_1 in the chamber is E_1 and the mean residual energy E_2 is the decreased energy of the particle after traversing the chamber at the pressure P_2 ($\Delta P = P_2 - P_1$; $E_2 < E_1$).

3.3 Bethe's Theory.- (See reference 14) Bethe's theoretical treatment of the energy loss is based on Born's approximation, applied to the collision between the heavy (alpha) particle and the atomic electrons. In this theory the differential cross section for the process in which the alpha particle transfers a given amount of energy to the atomic electrons is given by the square of the matrix element of the coulomb interaction between appropiate initial and final states. Plane waves are used for the wave functions of the incident and scattered alpha particle, the kinetic energies being E and E' (E'<E), respectively.

The condition of the atom is described initially by the unperturbed atomic wave function for the ground state and finally by the wave function for one of the excited states. Multiplying the cross section for a given energy loss by the energy lost and summing over all possibilities gives the final expression for the average energy lost per centimeter of path.

Use of the Born approximation requires that the amplitude of the wave scattered by the field of the atomic electron shall be small compared to the amplitude of the undisturbed incident wave. As it is well known the criterion for this is that:

$$\frac{ze^2}{\hbar v} \ll 1 \tag{3.15}$$

where ze and v are the charge and velocity of the primary particle, respectively and $\hbar$ is the Planck's constant. This condition is well satisfied for large velocities and small charge of the incident particle. Equation (3.15) is also, essentially the condition for the particle to have its full charge; when Eq. (3.15) is not fulfilled, the particle begins to capture electrons. The calculation of the stopping power is made much simpler if the velocity of the incident particle not only fulfills Eq. (3.15) but is in addition, large compared with the velocities of the electrons within the atoms, i.e., if:

$$E \gg \frac{M}{m} E_{el} \tag{3.16}$$

where E is the energy of the incident particle, E_{el} the ionization potential of the electrons, and M and m the masses of the incident particle and the electron, respectively.

Under these conditions and for non-relativistic velocities the average energy loss per centimeter of path or "stopping power" is:

$$-\frac{dE}{dx} = \frac{4\pi e^4 z^2}{mv^2} NB \tag{3.17}$$

with:

$$B = Z \log \left(\frac{2mv^2}{I}\right) \tag{3.17a}$$

Here v is the velocity and ze the charge of the incident particle, N the number of atoms per cubic centimeter of the material, Z the nuclear charge, I the average excitation potential of the atom, and the dimensionless logarithmic term B the "stopping number".

For relativistic velocities of the incident particle it is shown by Bethe that:

$$B = Z \left\{ \log \frac{2mv^2}{I} - \log (1 - \beta^2) - \beta^2 \right\} \tag{3.18}$$

where $\beta = v/c$ and c is the velocity of light. Although Equations (3.17) and (3.18) were derived for simple "hydrogen-like" atoms, it can be applied to other absorbers by adjusting I. The value of I is best determined from known range-energy data, from which it is found that I (given in electron volts) is related to Z by:

$$\begin{aligned} I &\sim 11.5\ Z \qquad \text{for } Z \leq 30 \\ I &\sim 8.8\ Z \qquad \text{for } Z > 30 \end{aligned} \tag{3.19}$$

From Equation (3.17) the following relationships are evident:

(a) Stopping power is proportional to electron density of the medium (NZ),

(b) Stopping power is proportional to the square of the charge of the incident particle; e.g., the stopping power for protons is 1/4 that for alpha particles having the same velocity. (Velocities are the same for protons having 1/4 the energy of alpha particles),

(c) Stopping power increases with decreasing particle velocity.

CHAPTER IV

EXPERIMENTAL ARRANGEMENT AND PROCEDURE

4.1 Detection System Description.- A block diagram of the detection system used in this project is given in figure 4.1. A mechanical vacuum pump was used to lower the pressure in the chamber. The pressure within the chamber was measured with a mercury manometer. Leakage of stopping gas into the chamber was controled by a manifold. An alpha source source was placed opposite a semiconductor detector in the gas chamber. The number of molecules along the path of the particle which provide the energy loss mechanism (coulombic interactions with the electrons) was varied by changing the gas pressure in the chamber. The residual energy of the alpha particles after traversing the separation distance between the source and detector, at a known gas temperature and pressure, is determined from the alpha spectra obtained from an analyzer system consisting of a semi-conductor (Si) detector, a bias power supply, a pulser, a preamplifier, an amplifier and a multichannel pulse height analyzer.

A general picture of the laboratory set-up is shown in figure 4.2 and a gas chamber close-up can be seen on figure 4.3. The alpha particle source used in this experiment was a calibrated 0.1 microcurie Am^{241} source, which had a negligible self-absorption and a minimum backscattering. This alpha source decays by emitting a 5.477-Mev alpha particle 84.2 percent of the time and this energy was assumed for all particles emitted. Several other energies were 5.433-Mev (13.6

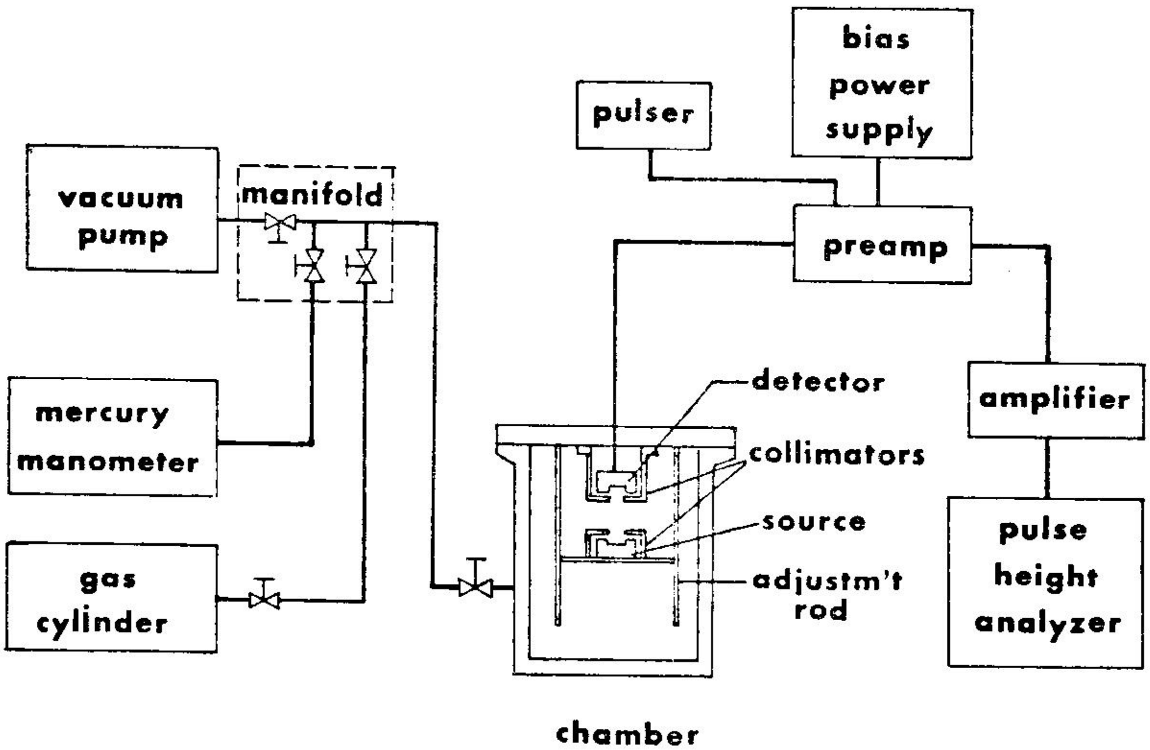

Figure No. 4.1 : Schematic diagram of the experimental arrangement.

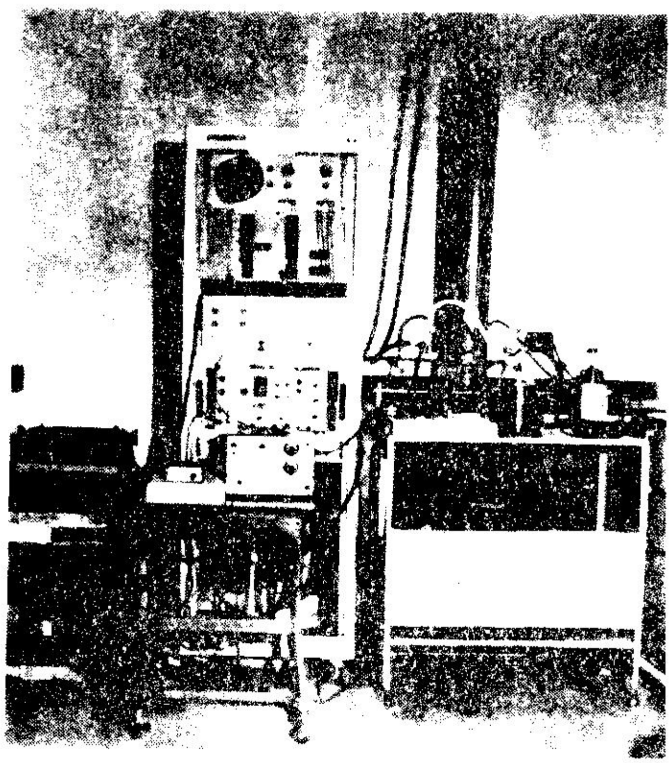

Figure 4.2 : Experimental set up for stopping power and range measurements.

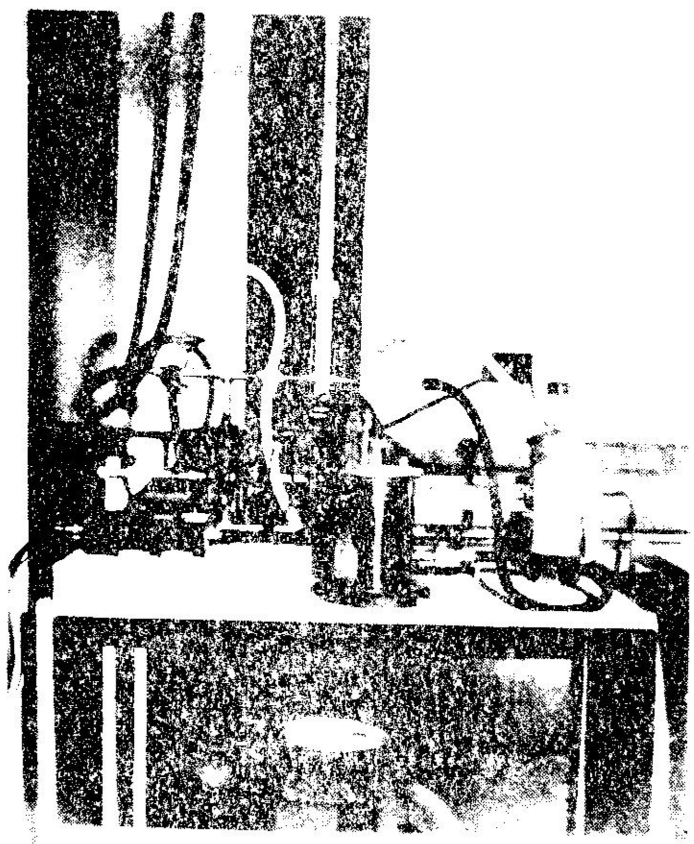

Figure 4.3 : Close up picture of the experimental set up.

percent) and 5.379-Mev (1.4 percent). The detector used was of the silicon surface-barrier type with sensitive area of 1 cm^2 and a typical insensitive thickness or dead layer of approximately 200 Angstroms [6] which was due almost entirely to the gold electrode on the surface. A graph of energy loss in the dead layer vs. alpha particle energy was constructed using the linear stopping power of gold for alpha particles[1] multiplied by the dead layer thickness. The graph showed that a 5.5, 1.0 and 0.2 alpha particle incident on the detector suffered an energy loss in penetrating the dead layer of 10, 15 and 8 Kev, respectively. Thus, the detector was essentially free of complicating "window" effects. It has been shown[5] that the response of solid state detectors are linear for alpha particles over the energy range of our experiment.

The source and the detector were mounted in line within the chamber and the separation distance could be varied by means of an adjustable rod upon which the source is mounted. Source and detector are shown in figure 4.4. Also, an aluminum collimators were placed over the alpha source and the detector in order to get a collimated beam of alpha particles.

4.2 Energy Loss Measurement.- The calibration factor in Kev/channel for the energy analyzing system was obtained by means of a pulser observing first the zero energy position and then by observing the location of the 5.477-Mev alpha peak while the chamber was under vacuum. The calibration curve and factor obtained is shown in figure 4.5. The calibration factor (7.77 Kev/channel) was also measured after

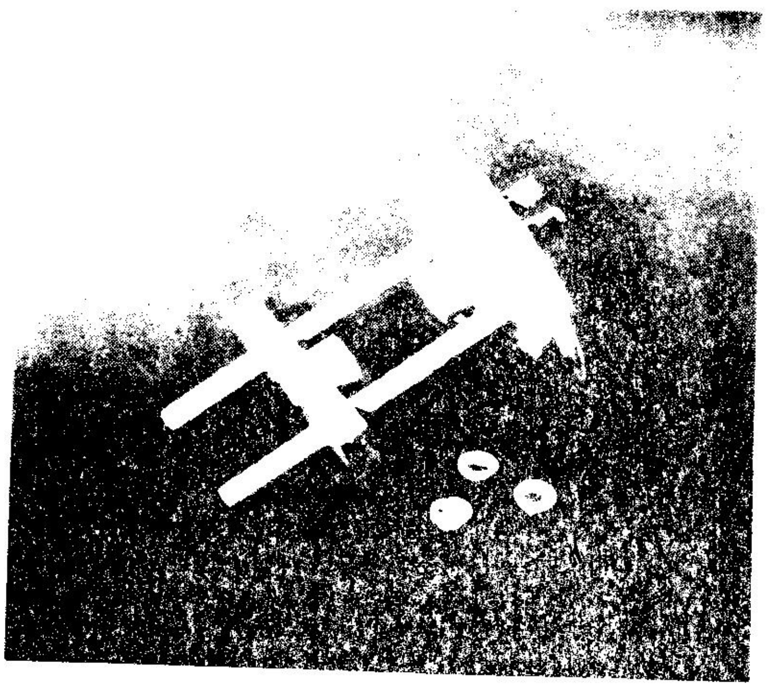

Figure 4.4 : Vacuum chamber inside instrumentation.

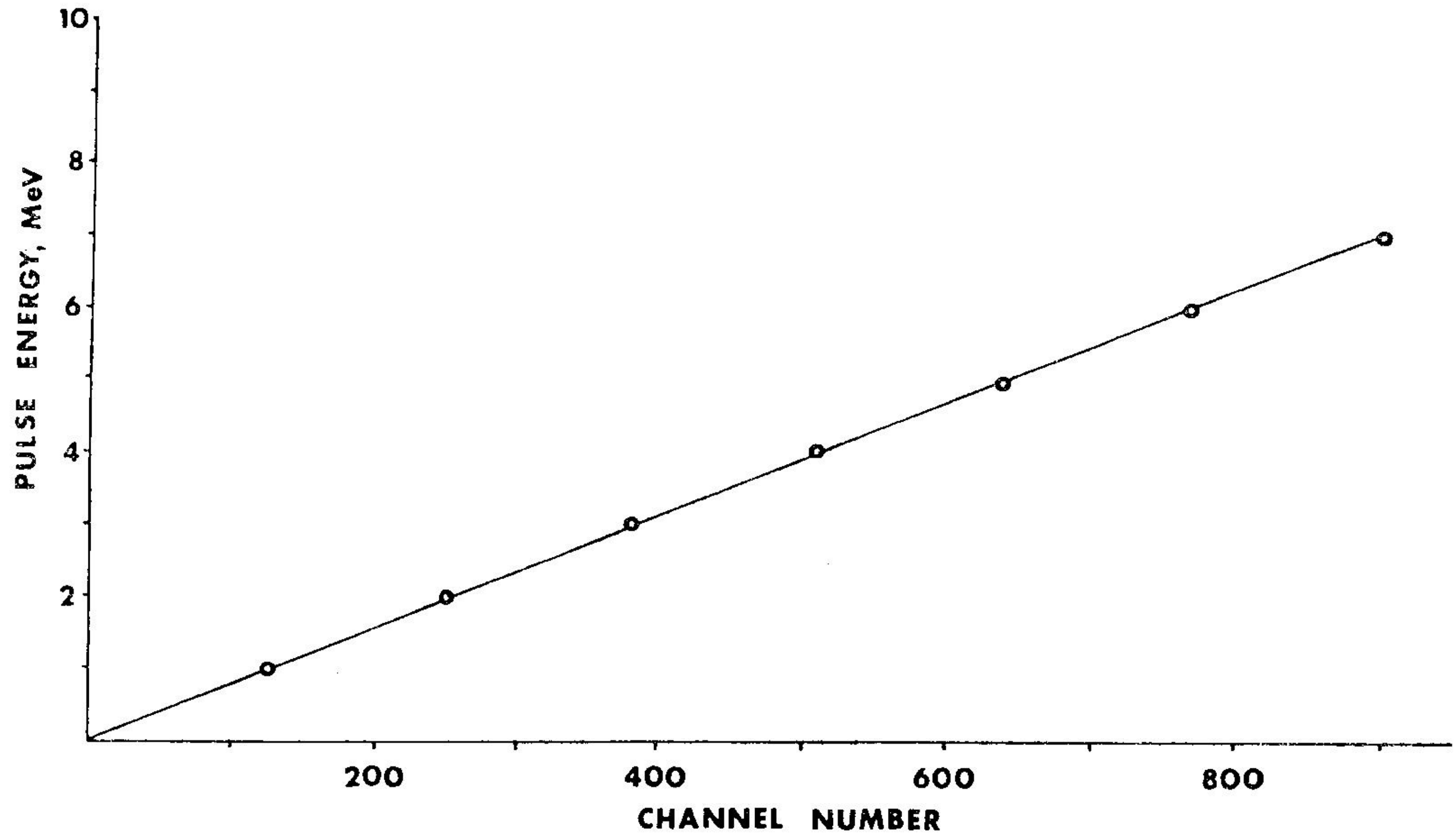

Figure 4.5 : Calibration curve for the stopping power measuring system, obtained by means of an energy pulser and a 1024 channel energy analyzer. Calibration factor obtained was 7.77 Kev/channel.

each set of energy loss measurements. No significant drifts were observed in the zero energy position. The temperature of the laboratory was maintained within 1°F of a mean temperature (75°F) so that it was possible to average several sets of energy loss measurements on each gas.

Using the 5.477 Mev Am^{241}-alpha particle and a fixed source-detector distance, energy spectra at several different pressures were taken for each of the gases considered. Information on the gases used on the experiments in given in Table 4.1, and an example of several energy spectra of alpha particles after traversing 5.4 cms of air at various gas pressures and at 24°C is shown on figure 4.6. Multiplying the calibration factor (Kev/channel) by the channel number of the alpha peak, we found the averaged peak energy of the alpha particles reaching the detector after traversing through the stopping gas at a given chamber pressure. Using a simple relationship from Eq. (3.12) we get an expression for calculating the equivalent distance at standard conditions (X_{stp}) corresponding to the distance traversed by the alpha particle at chamber conditions. In other words,

$$X_{stp} \frac{Po}{To} = d. \frac{Pch}{Tch} \tag{4.1}$$

where the subscripts "o" and "ch" mean standard and chamber conditions respectively, and d is the separation distance between the alpha source and detector within the chamber. The last expression

TABLE 4.1

SOME CHEMICAL AND PHYSICAL PROPERTIES OF GASES USED IN THIS WORK

GAS	STRUCTURE[1]	MOLECULAR WEIGHT[2] M (gm/mole)	STANDARD DENSITY $_o$ (mg/cm^3)
AIR		28.97	1.293
A		39.95	1.789
N_2	: N ≡ N :	28.01	1.251
Kr		83.80	3.736
O_2	: Ö = O : [(a)]	31.998	1.429
CO_2	: O = C = O : [(b)]	44.01	1.977
N_2O	: N = N⁺ = O :		
Freon 14		170.92	7.036
CH_4	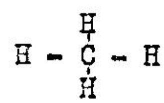	16.04	0.717
C_2H_4		28.05	1.252
C_2H_6	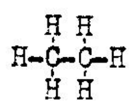	30.07	1.342
C_3H_6	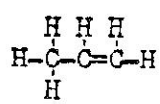	42.08	1.878
C_3H_8	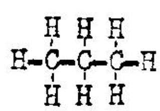	44.09	1.967

1: Given by Pauling[12], unless otherwise specified.
2: Given by Weast (15).
(a): Given by Orville-Thomas[10]
(b): Given by Bent (2).

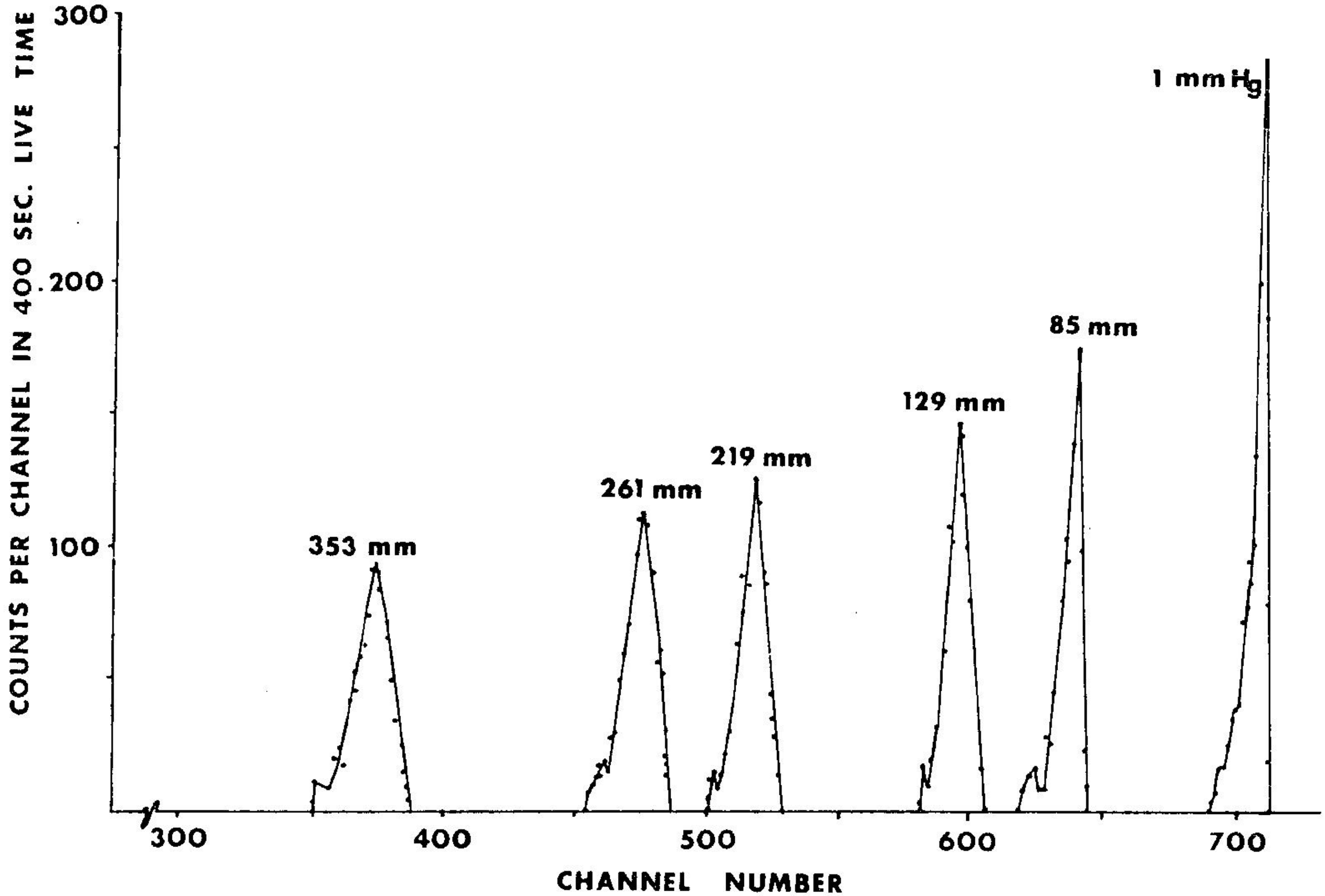

Figure 4.6: Several energy spectra of alpha particles after traversing 5.4 cms of air at various gas pressures and at 24°C.

may be rearranged as it follows :

$$X_{stp} = d \cdot \frac{Pch}{Po} \qquad (4.1a)$$

assuming that the temperature quotient (To/Tch) is approximately equal to unity.

Experimental energy and chamber pressure data for each of the gases mentioned in Table 4.1 were taken by varying the gas pressures on the chamber at intervals of 1 to 10 centimeters of mercury and the results were plotted in figures 4.7, 4.8 and 4.9. By differentiating graphically these curves, the stopping power parameters were calculated taking $\Delta x = 1$ mm. and an average value for the corresponding energy. In other words, if $\Delta E = E_2 - E_1$, $E_{aver} = (E_1 + E_2)/2$. Finally, the stopping power ($- dE/dx$) was plotted against E_{aver} for each gas. The results are given in figures 4.10 to 4.13.

Ranges of alpha particles with energies between 2.60 and 5.47 Mev were determined simultaneously with the stopping power measurements by counting the number of alpha particles of a certain energies reaching the detector in a fixed period of time at a given gas pressure. In order to decrease alpha energies, very thin metal foils (Cu: 0.00004" and 0.00012"; Ti: 0.00015" and 0.0002" thick) were placed over the 5.47-Mev alpha source and the energy peaks coming from the decreased energy particles shown acceptable broadening averaging 5.04, 4.84, 4.23, 4.02, 3.53, 3.27 and 2.60 Mev obtained using individual and combined metal foils. Air and hydrocarbon gases were

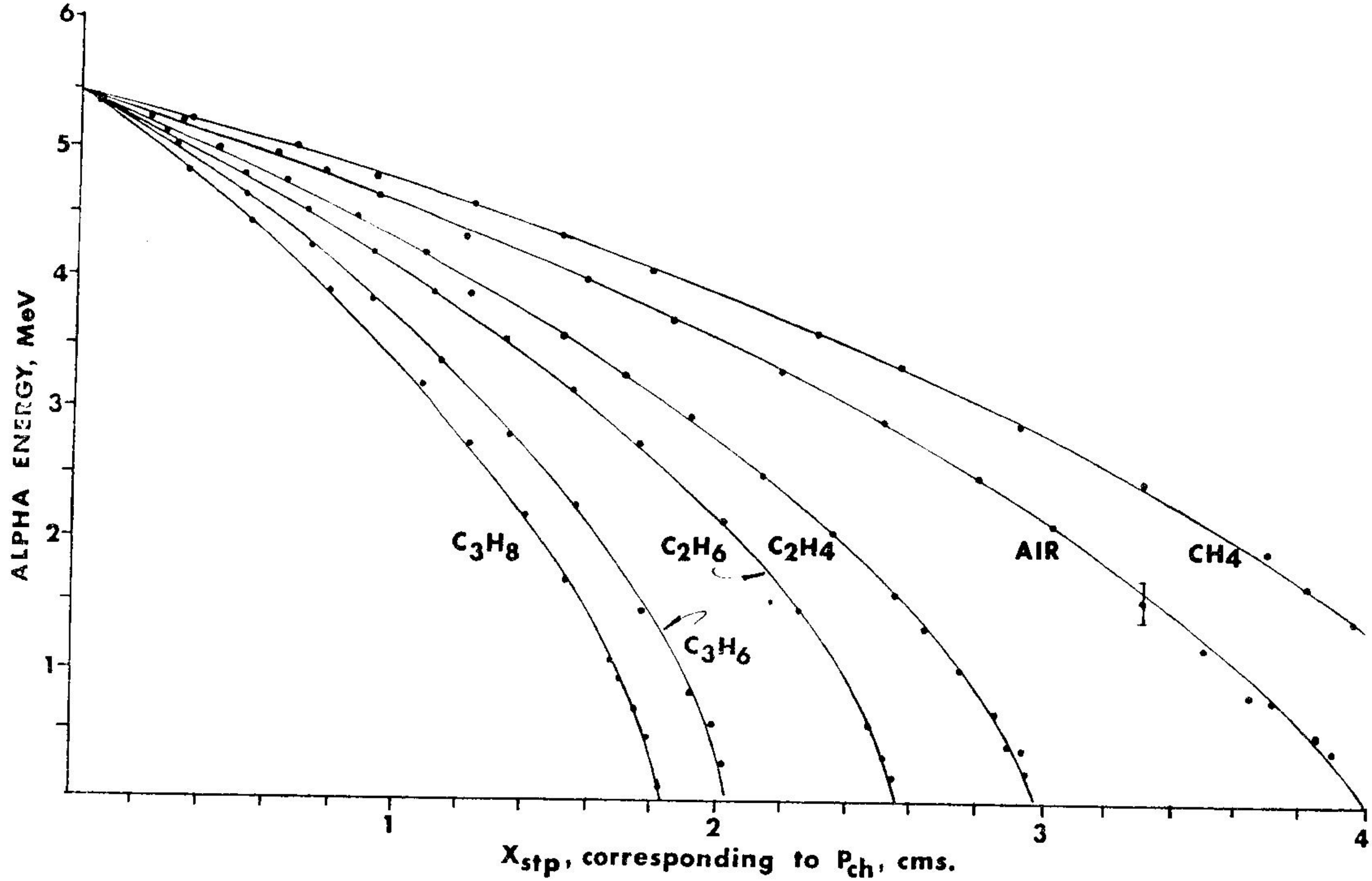

Figure 4.7 : Remaining energy of 5.47 Mev Am^{241} alpha particles after traversing a certain path X_{stp} , corresponding to the chamber gas pressure for air and hydrocarbon gases.

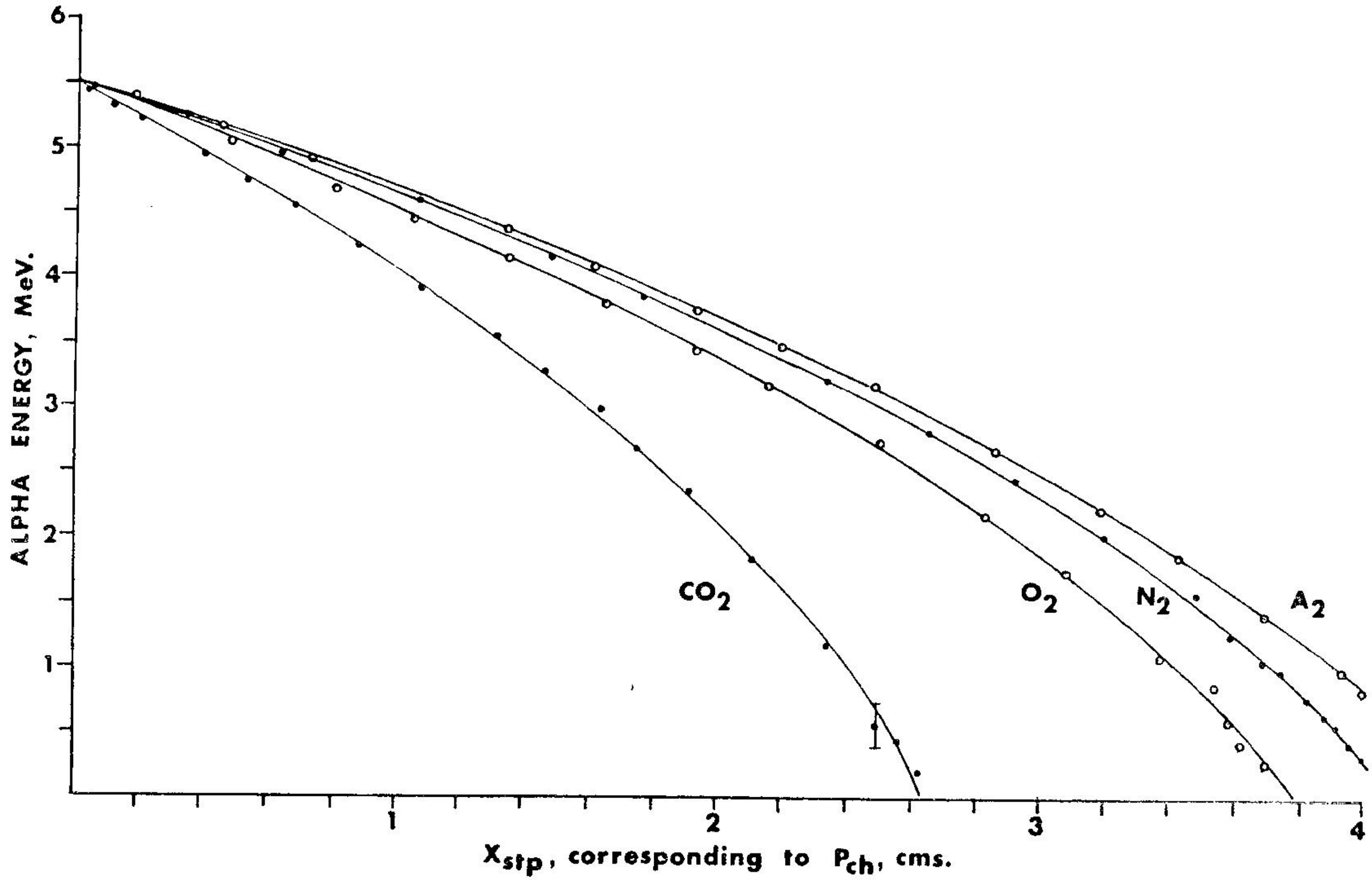

Figure 4.8 : Remaining energy of 5.47-Mev Am^{241} alpha particles after traversing a certain path X_{stp}, corresponding to the chamber gas pressure for A, N_2, O_2 and CO_2.

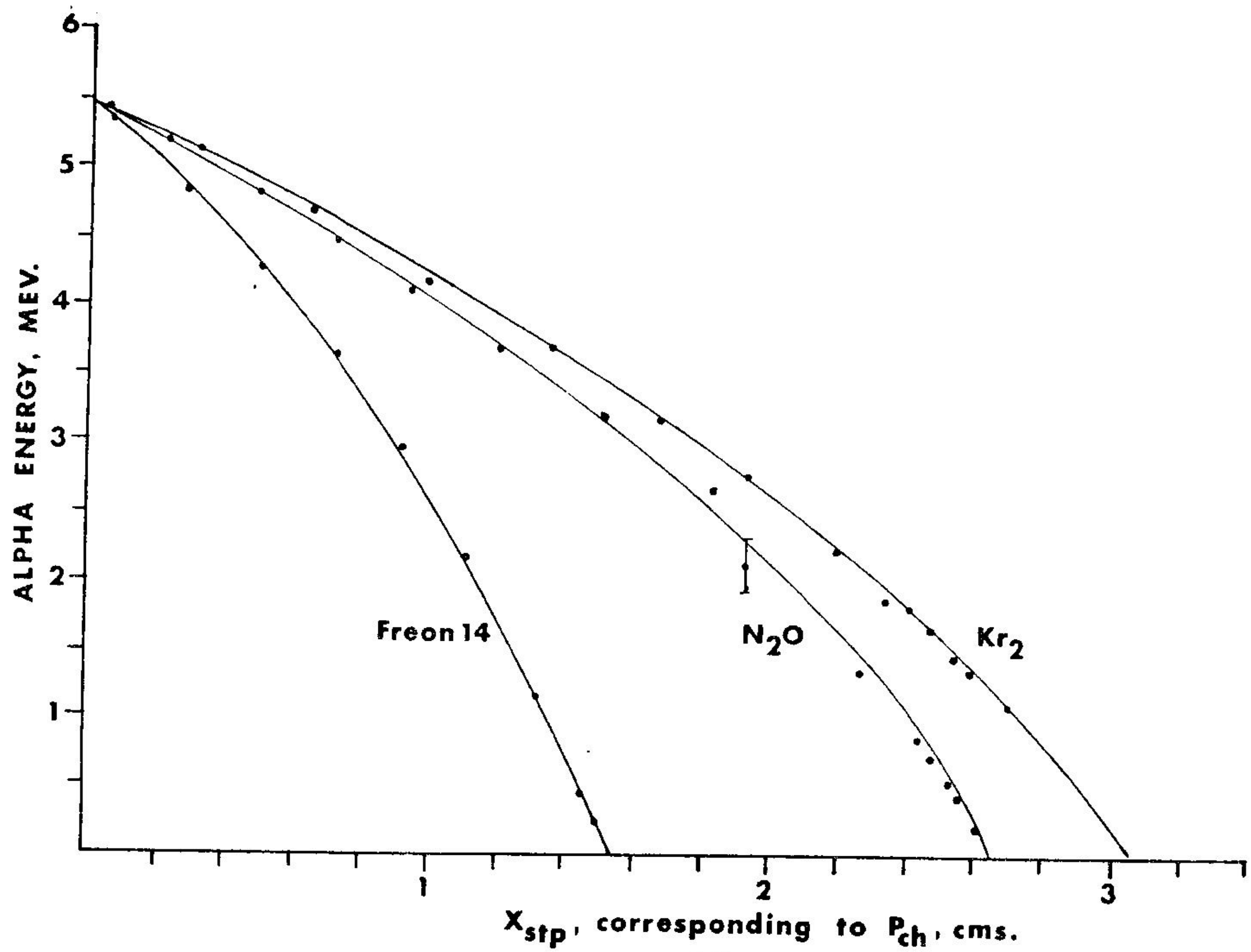

Figure 4.9 : Romainig energy of 5.47-Mev Am^{241} alpha particles after traversing a certain path X_{stp}, corresponding to the chamber gas pressure for Kr_2, N_2O and Freon-14.

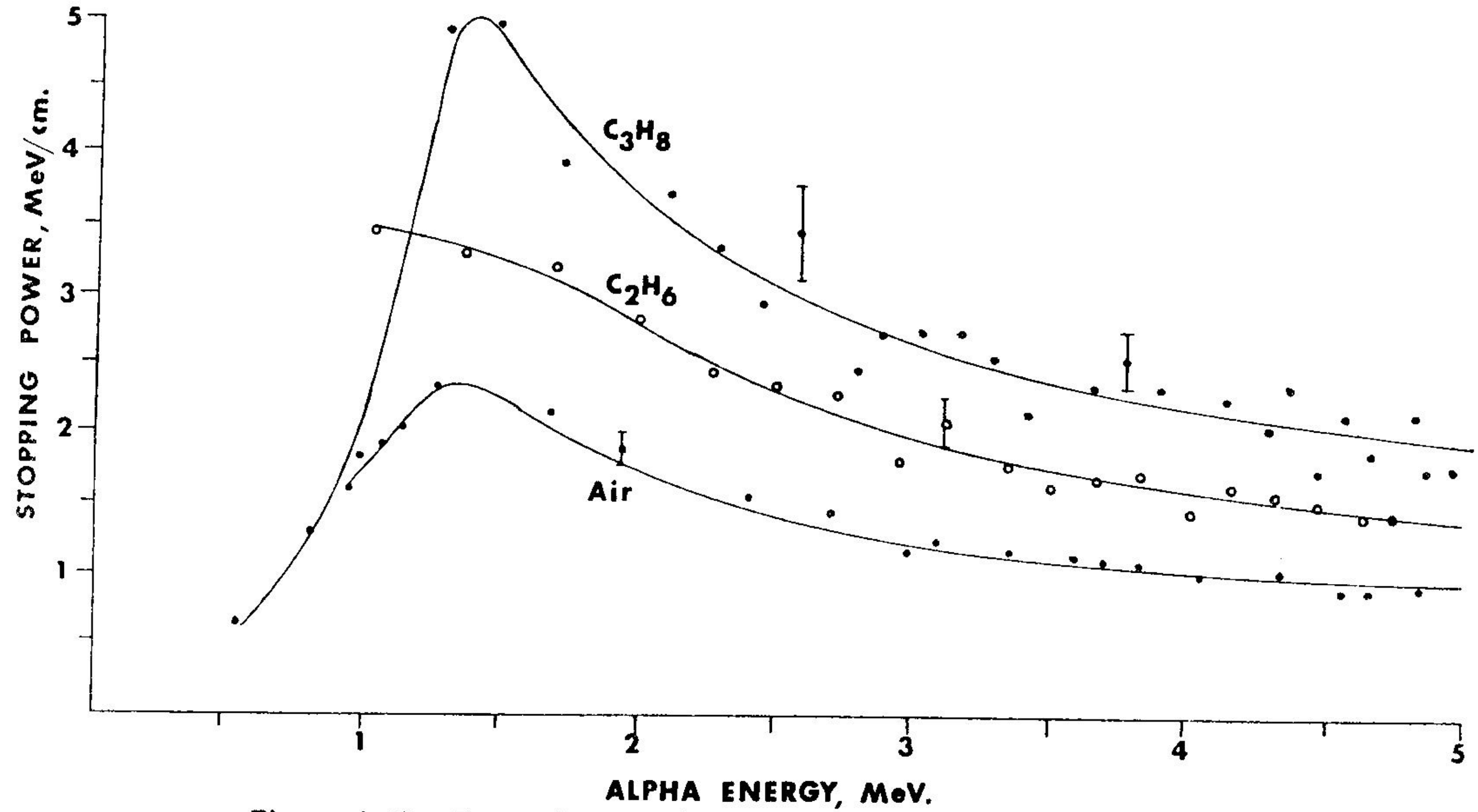

Figure 4.10 : Energy loss of alpha particles in air, C_2H_6 and C_3H_8.

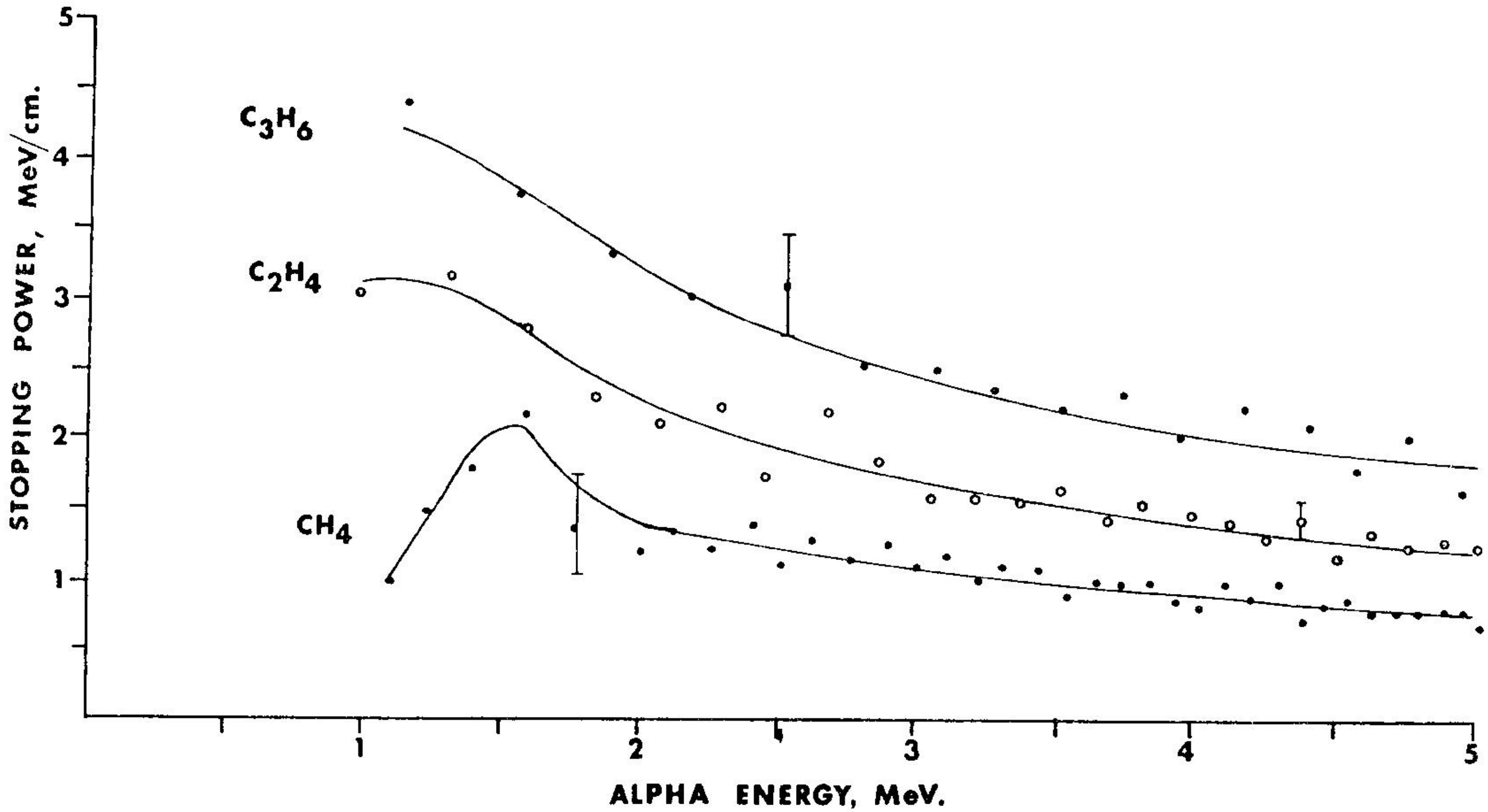

Figure 4.11 : Energy loss of alpha particles in CH_4, C_2H_4 and C_3H_6.

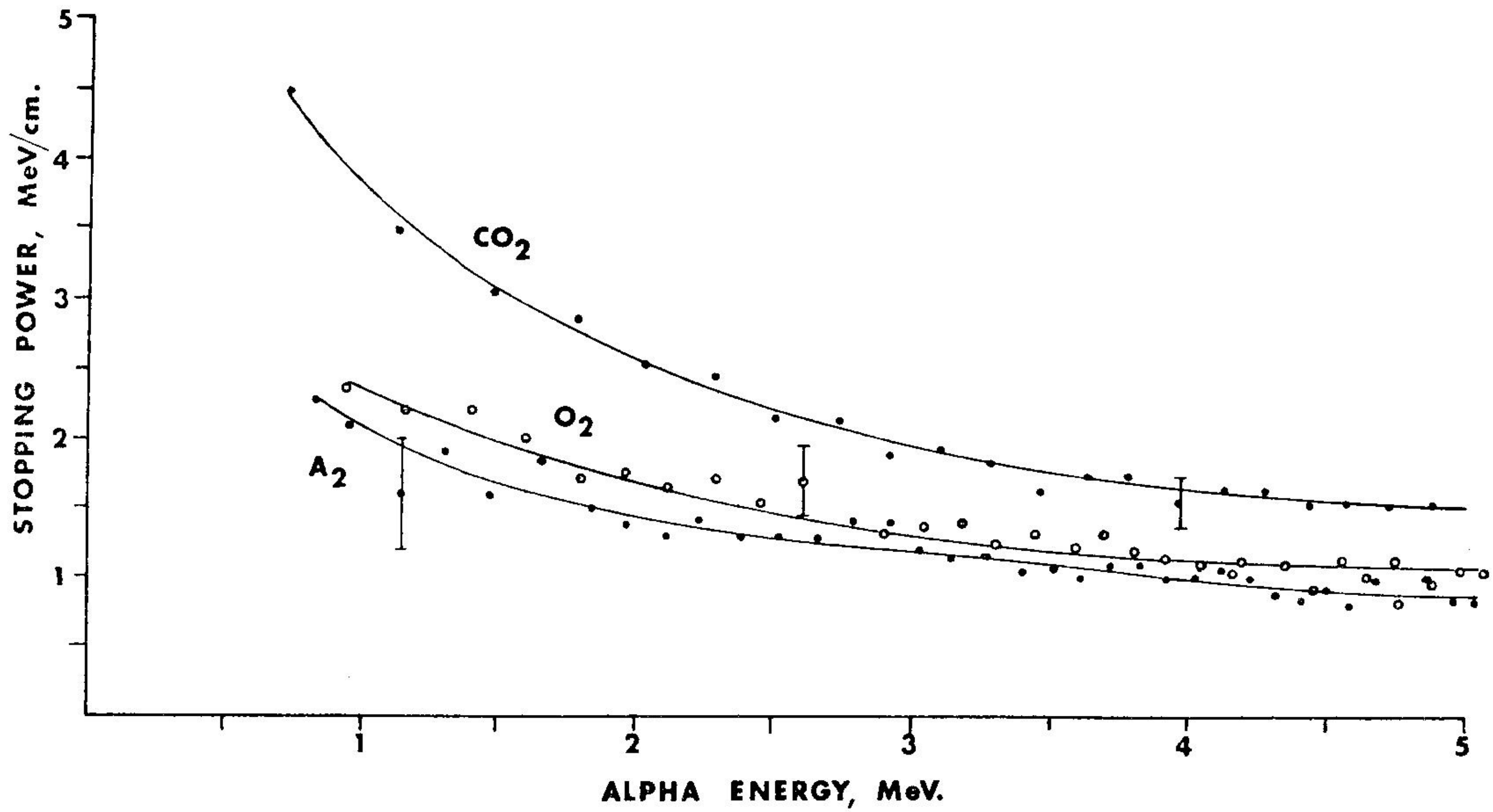

Figure 4.12 : Energy loss of alpha particles in A_2, O_2 and CO_2.

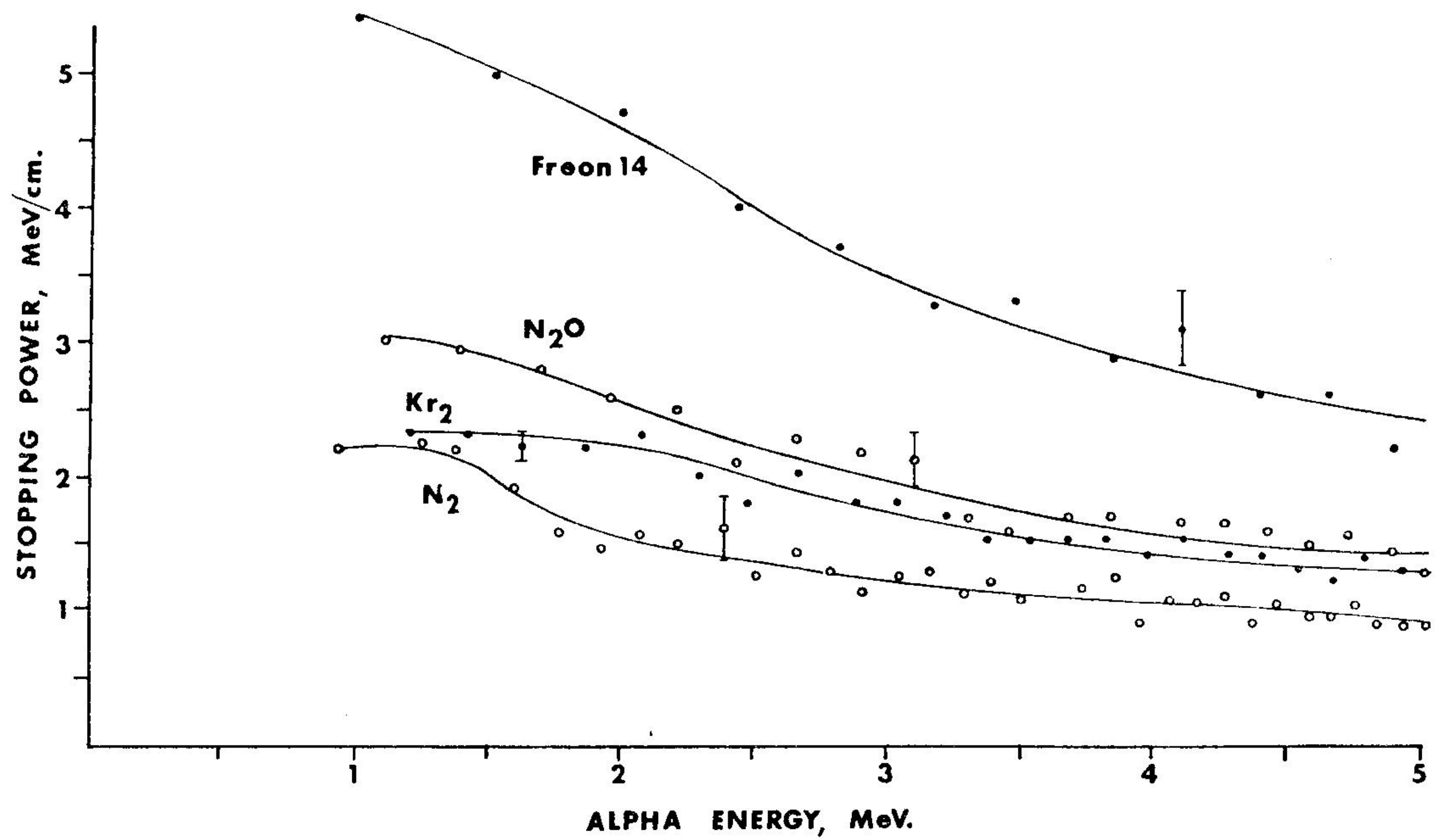

Figure 4.13 : Energy loss of alpha particles in N_2, Kr_2, N_2O and Freon 14.

chosen for this part of the experiments and the results are tabulated on Table 4.2 and plotted on Figures 4.14 to 4.20. Adittional range data for other gases such as O_2, N_2, CO_2, A_2, Kr_2, N_2O and Freon-14 is presented on Figures 4.21 and 4.22 for 5.47-Mev alpha particles. Range curves were calculated by normalizing the total counts using the ratio of total counts and maximum total counts recorded by the scaler for the same period of time. Table A.1 (see Apendix) is a record of the settings of the instruments used on the experimental measurements.

4.3 Cross Section Calculations.- Molecular cross sections for air and hydrocarbon gases (CH_4, C_2H_4, C_2H_6, C_3H_8, C_3H_6) were calculated by means of Equation (3.14) and the following constant values:

Avogadro's number (A): 6.024 x 10^{23} molecules/gram mole

Standard Temperature (T_o): 273°K

Standard Pressure (P_o): 760 mm of mercury.

Source to detector distance (d): 5.4 cms.

Molecular weight and standard density values for each gas to be inserted on Equation (3.14) are given in Table 4.1. Cross Sections for air, methane, ethane, propane, ethylene and propylene for 0.3 - 5.0 Mev alpha particles are tabulated on Table 4.3, and curves of molecular cross sections (10^{-14} ev/molecule/cm2 versus alpha energy (Mev) were drawn in Figures 4.23 and 4.24.

TABLE 4.2

RANGE-ENERGY RELATIONSHIP OF AIR AND HYDROCARBON GASES FOR ALPHA PARTICLES*

ALPHA PARTICLE ENERGY, MeV	RANGE, CMS					
	AIR	CH_4	C_2H_4	C_2H_6	C_3H_6	C_3H_8
5.47	3.89	4.27	2.96	2.56	2.05	1.85
5.04	3.53	3.74	2.38	-	1.57	1.48
4.84	3.32	3.52	2.13	2.00	1.51	1.35
4.23	2.73	-	1.63	1.42	1.11	1.00
4.06	2.63	2.42	1.53	1.35	1.03	0.98
3.53	2.10	1.92	1.19	1.06	0.92	-
3.38	-	-	-	-	-	0.72
3.27	-	1.78	-	-	-	0.70
2.60	1.41	1.11	0.69	0.68	0.62	-
1.43	-	-	-	-	-	0.13

* These values are plotted in Figure 4.20.

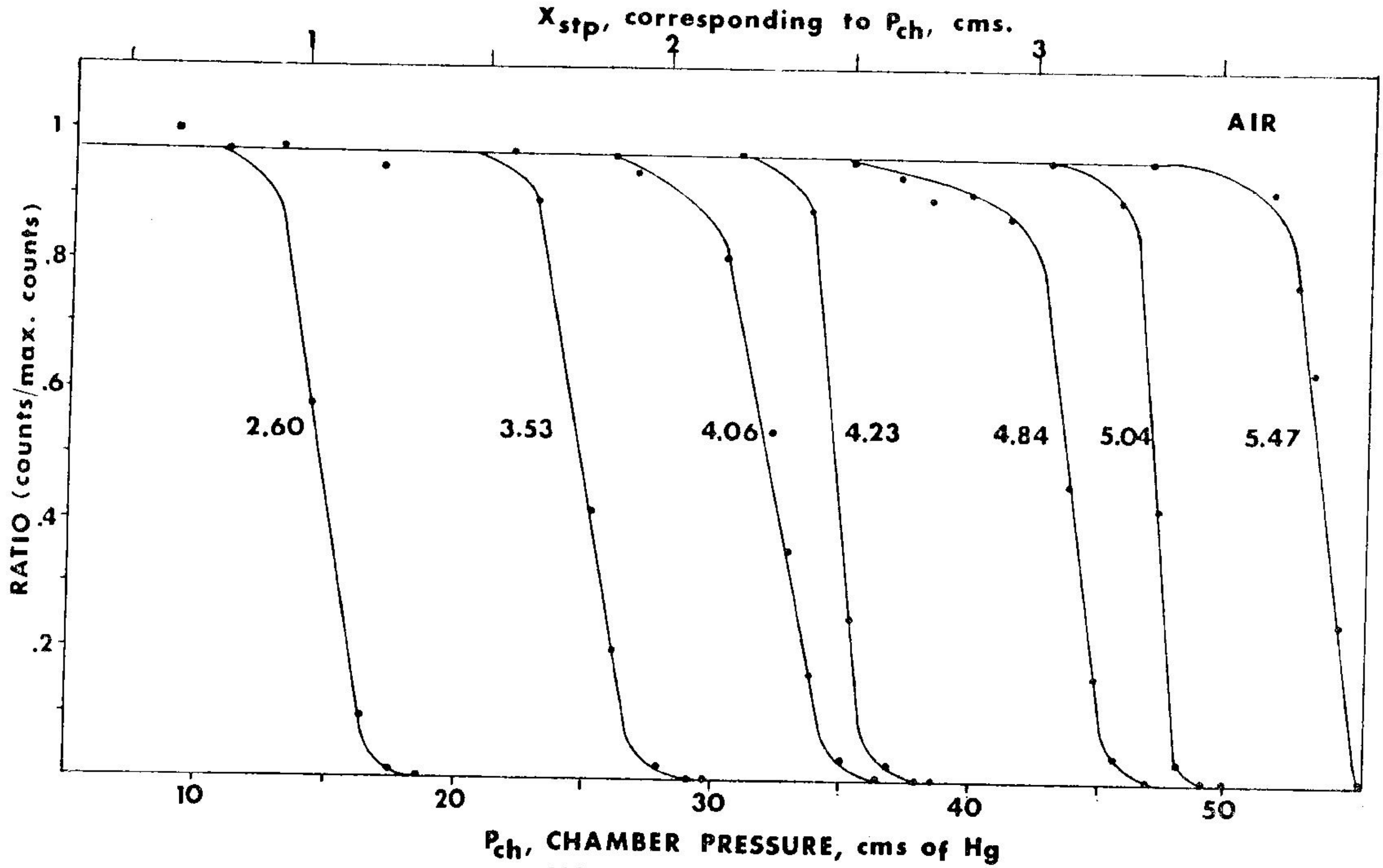

Figure 4.14: Range curves for the Am^{241} alpha particles (5.47 Mev initial kinetic energy) and for alpha particles after trespassing very thin Cu and Ti foils in air. Figures on the curves mean energy values, in Mev.

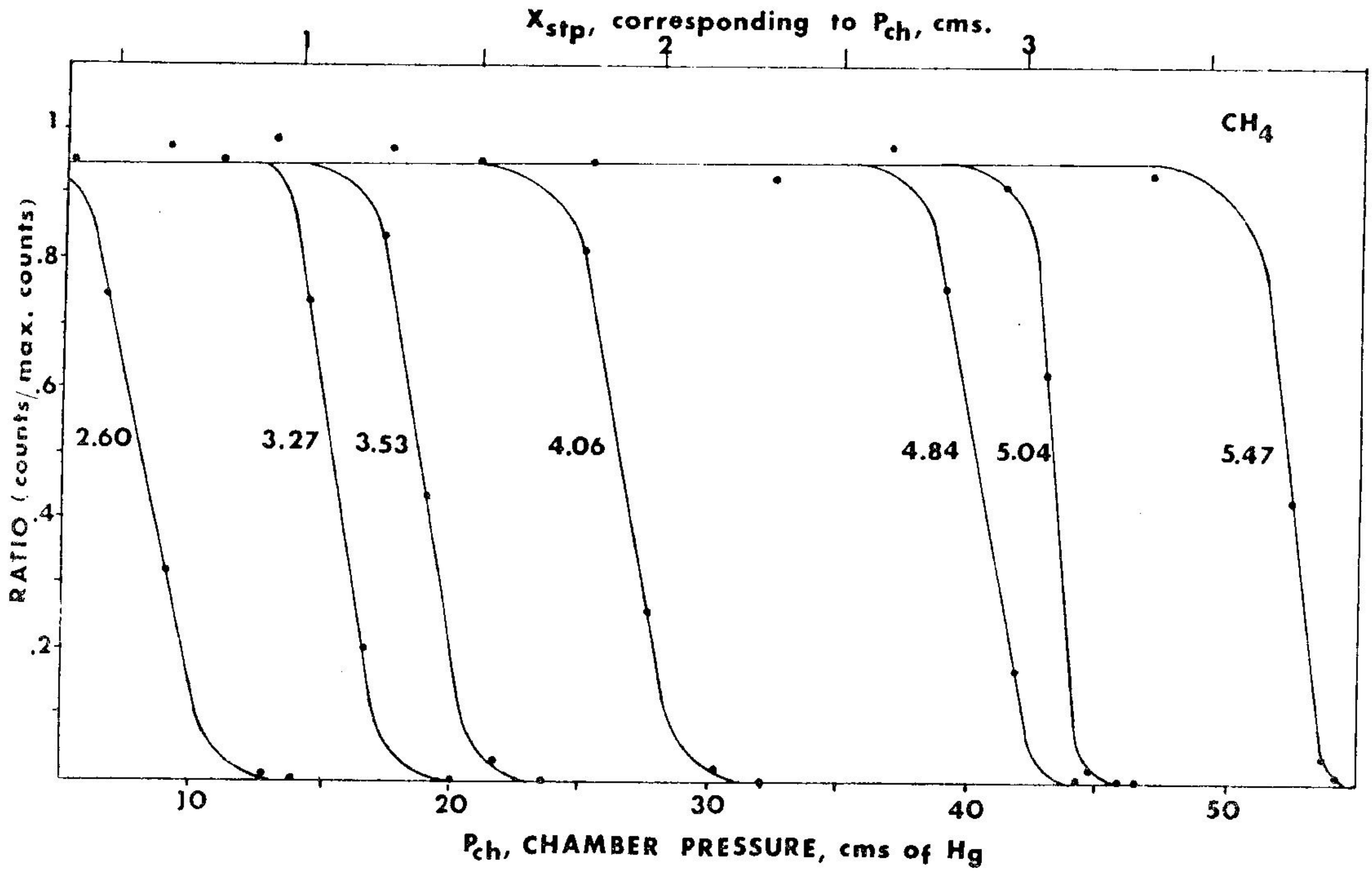

Figure 4.15 : Range curves for the Am^{241} alpha particles (5.47 Mev initial kinetic energy) and for alpha particles after trespassing very thin Cu and Ti foils in Methane (CH_4). Figures on the curves mean energy values, in Mev.

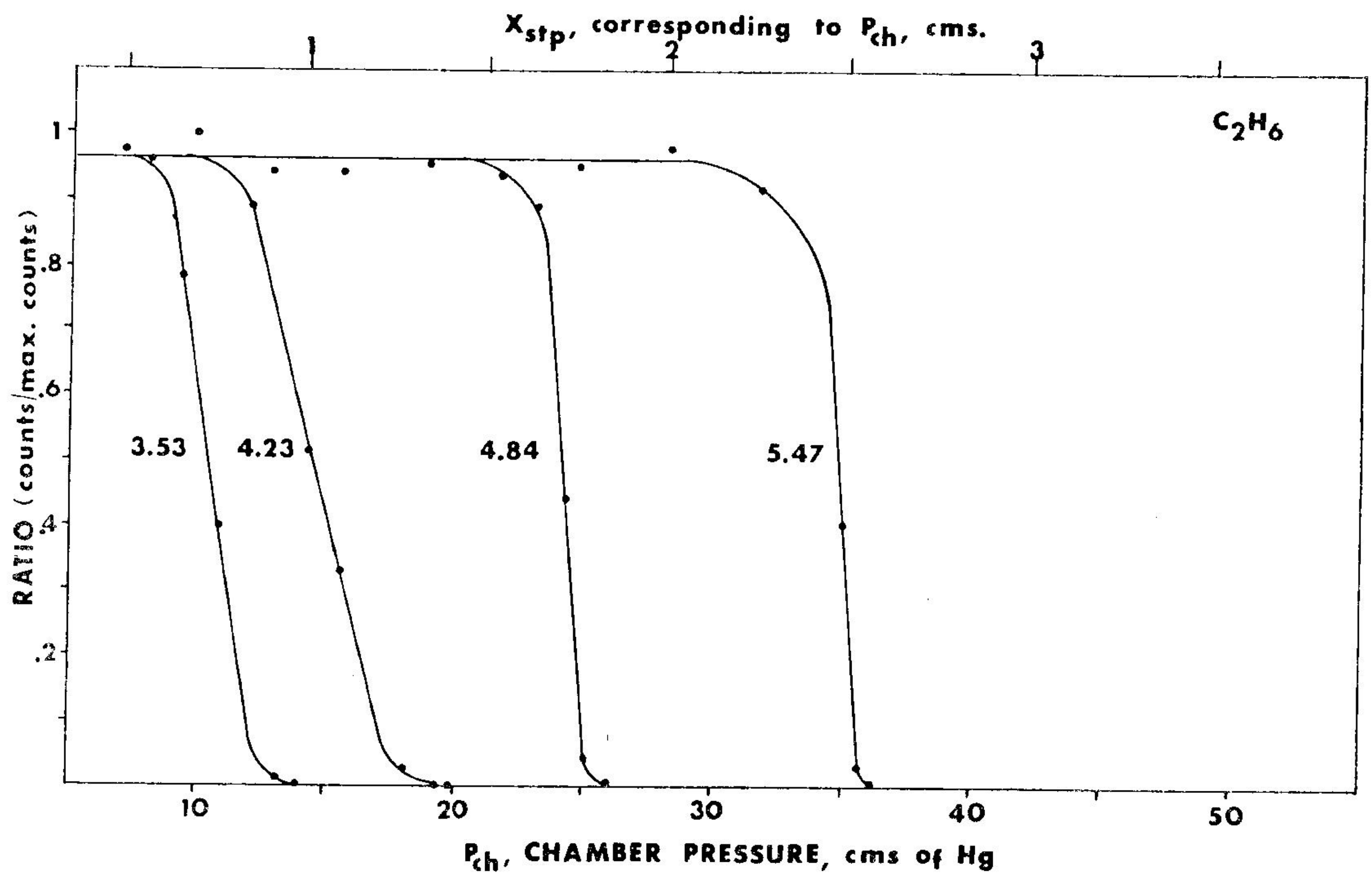

Figure 4.16 : Range curves for the Am^{241} alpha particles (5.47 Mev initial kinetic energy) and for alpha particles after trespassing very thin Cu and Ti foils in Ethane (C_2H_6). Figures on the curves mean energy values, in Mev.

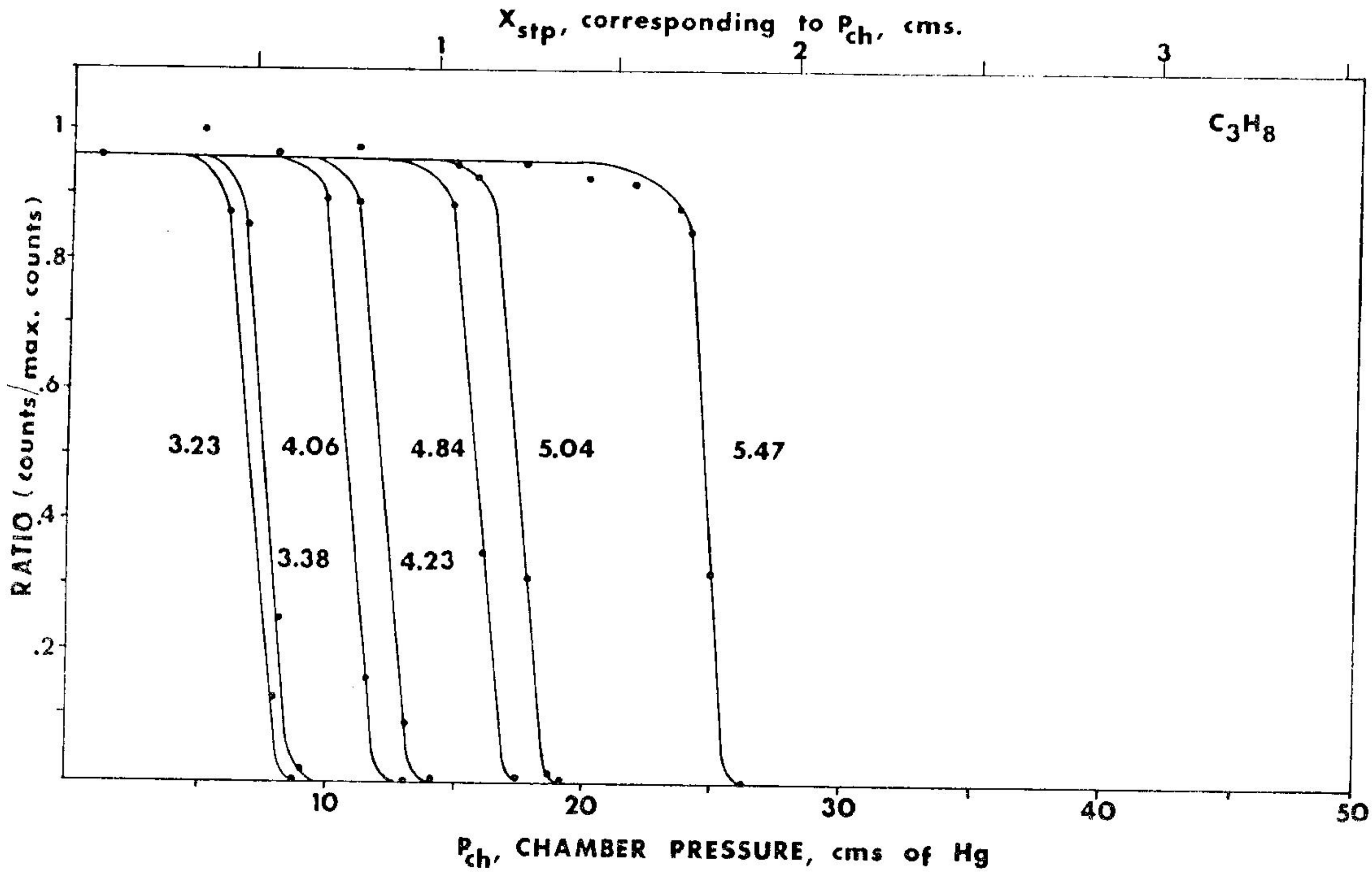

Figure 4.17 : Range curves for the Am^{241} alpha particles (5.47 Mev initial kinetic energy) and for alpha particles after trespassing very thin Cu and Ti foils in Propane (C_3H_8). Figures on the curves mean energy values, in Mev.

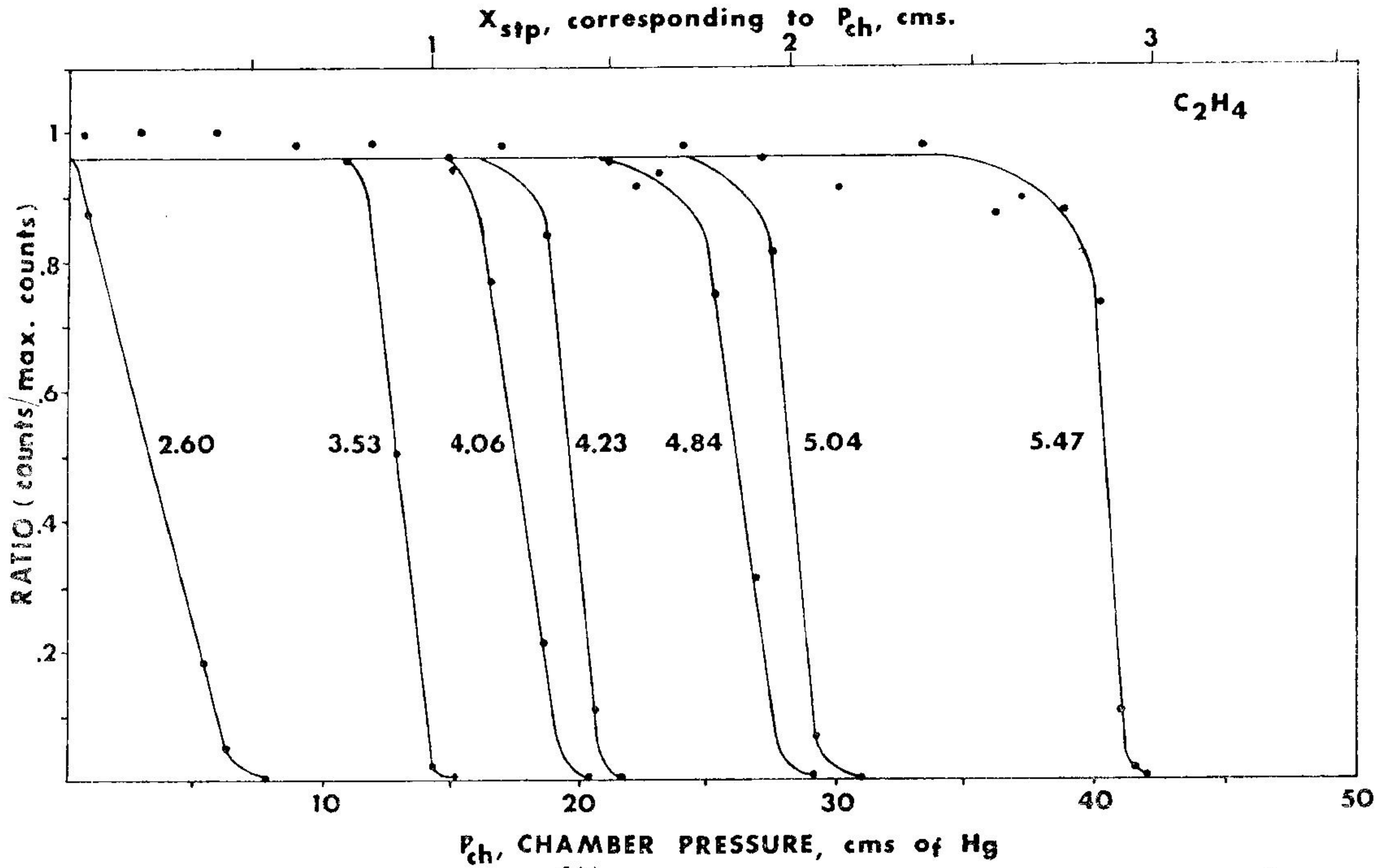

Figure 4.18 : Range curves for the Am^{241} alpha particles (5.47 Mev initial kinetic energy) and for alpha particles after trespassing very thin Cu and Ti foils in Ethylene (C_2H_4). Figures on the curves mean energy values, in Mev.

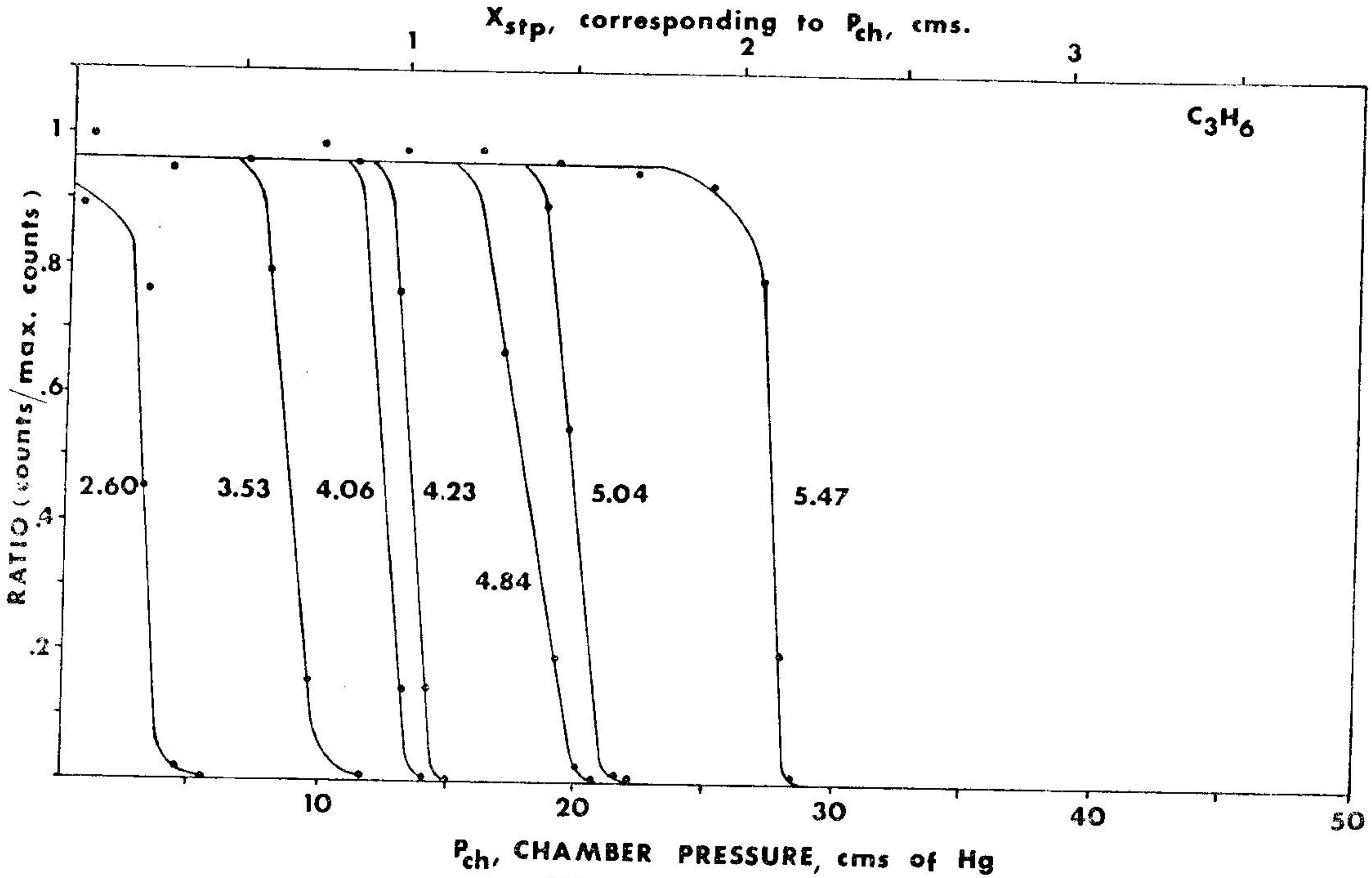

Figure 4.19: Range curves for the Am^{241} alpha particles (5.47 Mev initial kinetic energy) and for alpha particles after trespassing very thin Cu and Ti foils in Propylene (C_3H_6). Figures on the curves mean energy values, in Mev.

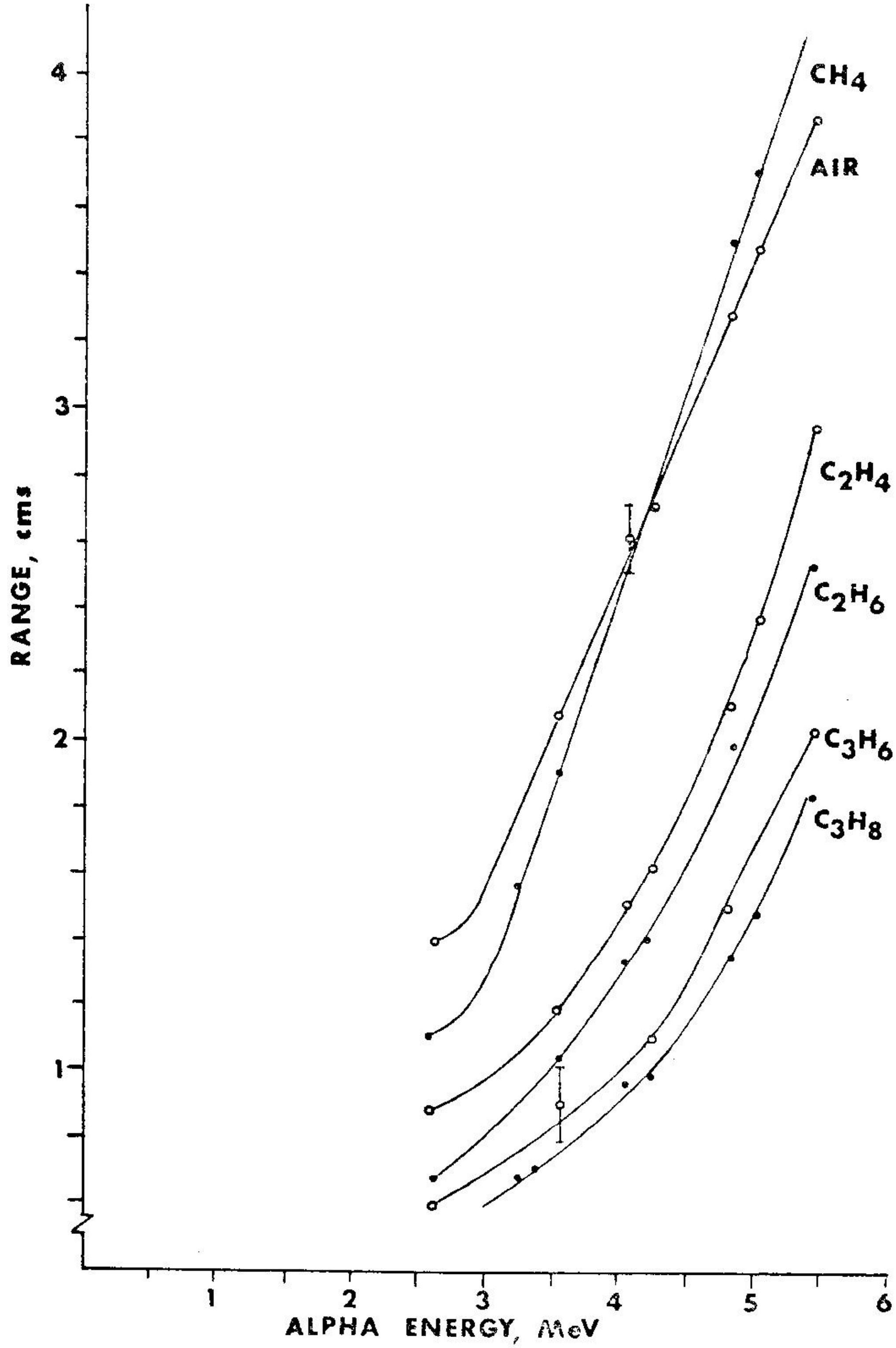

Figure 4.20 : Range-energy relation of slow alpha particles in air and hydrocarbon gases at standard condition.

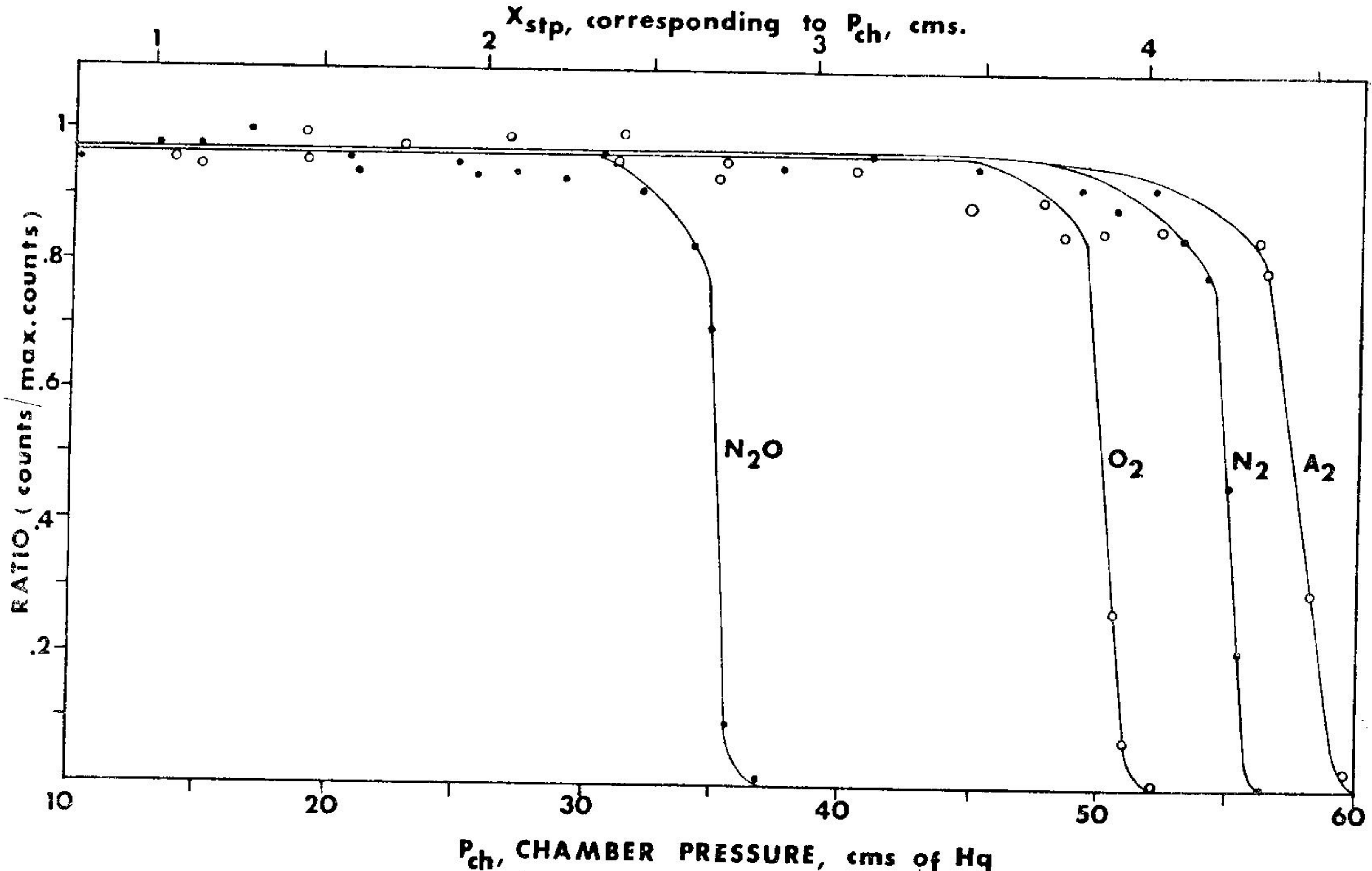

Figure 4.21 : Range curves for Am^{241} alpha particles (5.47 Mev) in several inorganic gases (A_2, N_2, O_2 and N_2O).

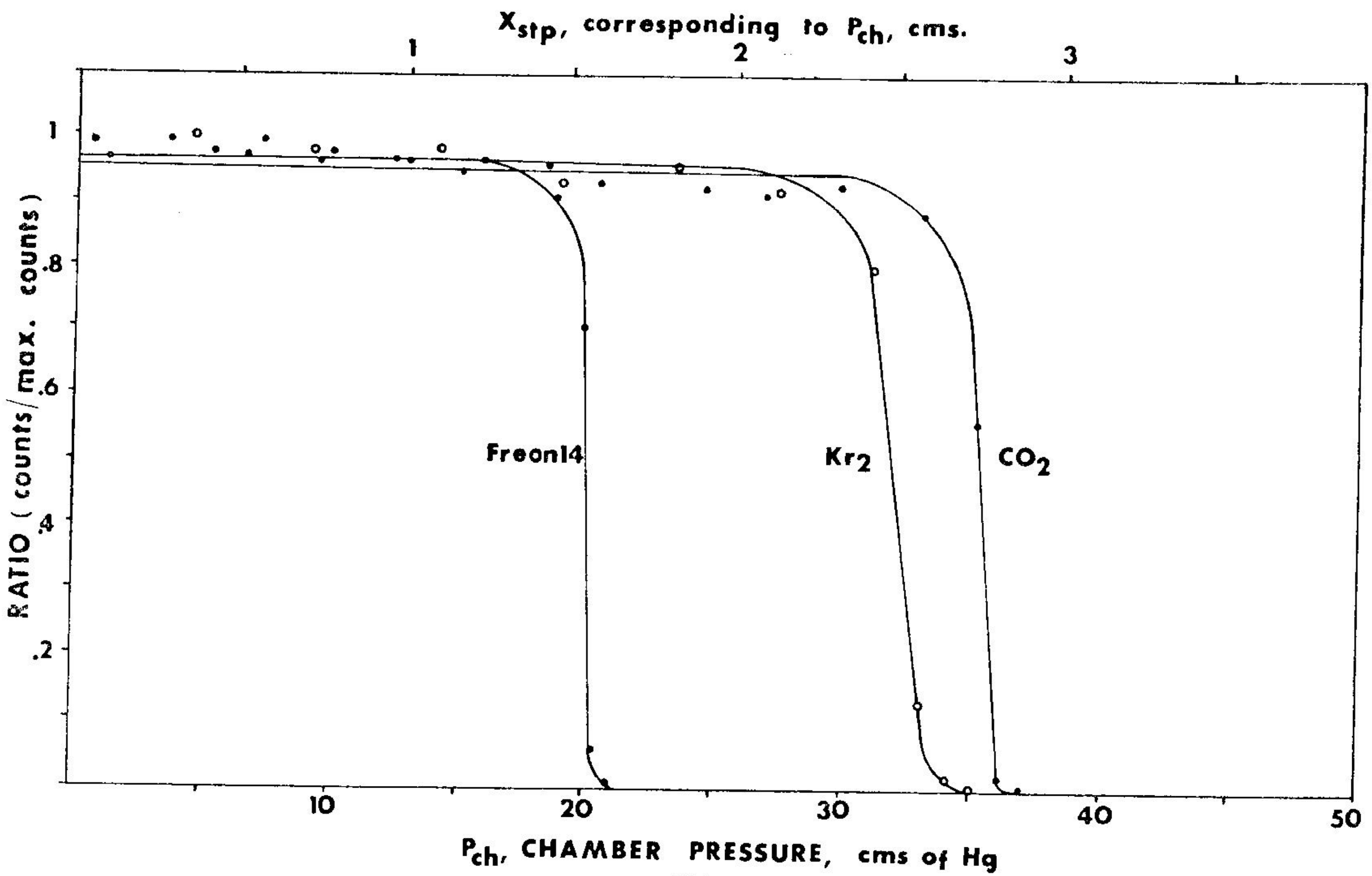

Figure 4.22 : Range curves for Am^{241} alpha particles (5.47 Mev) in CO_2, Kr_2 and Freon 14.

TABLE 4.3

MOLECULAR STOPPING CROSS SECTIONS OF AIR AND HYDROCARBON GASES FOR ALPHA PARTICLES*

ALPHA PARTICLE ENERGY, MeV	MOLECULAR STOPPING CROSS SECTION (10^{-14} ev/molecule/cm^2)					
	AIR	CH_4	C_2H_4	C_2H_6	C_3H_6	C_3H_8
0.3	-	-	13.5	19.6	23.5	26.0
0.4	-	-	16.0	21.3	28.5	27.0
0.5	5.5	-	17.2	22.5	27.1	27.5
0.6	6.2	-	17.5	23.0	24.5	27.6
0.7	6.9	11.1	16.5	22.5	23.0	27.0
0.8	7.7	10.0	15.5	21.0	21.5	26.0
0.9	8.5	9.0	14.7	19.5	20.4	24.8
1.0	9.2	8.5	13.8	18.5	19.1	24.0
1.2	9.9	7.5	12.5	16.0	17.5	22.6
1.4	10.0	6.8	11.3	14.2	15.9	19.3
1.6	9.5	6.3	10.4	12.7	14.7	17.4
1.8	8.7	5.9	9.6	11.6	13.7	16.0
2.0	8.0	5.5	8.9	10.6	12.7	14.6
2.2	7.2	5.2	8.4	9.8	12.0	13.7
2.4	6.5	5.0	7.8	9.1	11.2	12.8
2.6	5.9	4.7	7.4	8.5	10.7	12.0
2.8	5.5	4.5	7.0	8.0	10.1	11.4
3.0	5.1	4.3	6.7	7.6	9.7	10.9
3.2	4.7	4.1	6.5	7.2	9.3	10.5

CONT. TABLE 4.3

ALPHA PARTICLE ENERGY, MeV	MOLECULAR STOPPING CROSS SECTION (10^{-14} ev/molecule/cm^2) AIR	CH_4	C_2H_4	C_2H_6	C_3H_6	C_3H_8
3.4	4.5	3.9	6.2	6.9	8.9	10.0
3.6	4.3	3.8	6.0	6.7	8.6	9.7
3.8	4.1	3.6	5.8	6.5	8.3	9.4
4.0	3.9	3.5	5.6	6.3	8.0	9.0
4.2	3.8	3.3	5.4	6.1	7.8	8.7
4.4	3.7	3.2	5.2	5.9	7.6	8.6
4.6	3.7	3.1	5.0	5.7	7.4	8.4
4.8	3.6	3.0	4.9	5.6	7.3	8.2
5.0	3.5	2.9	4.8	5.5	7.1	8.0

* These values are plotted in Figures 4.23 and 4.24.

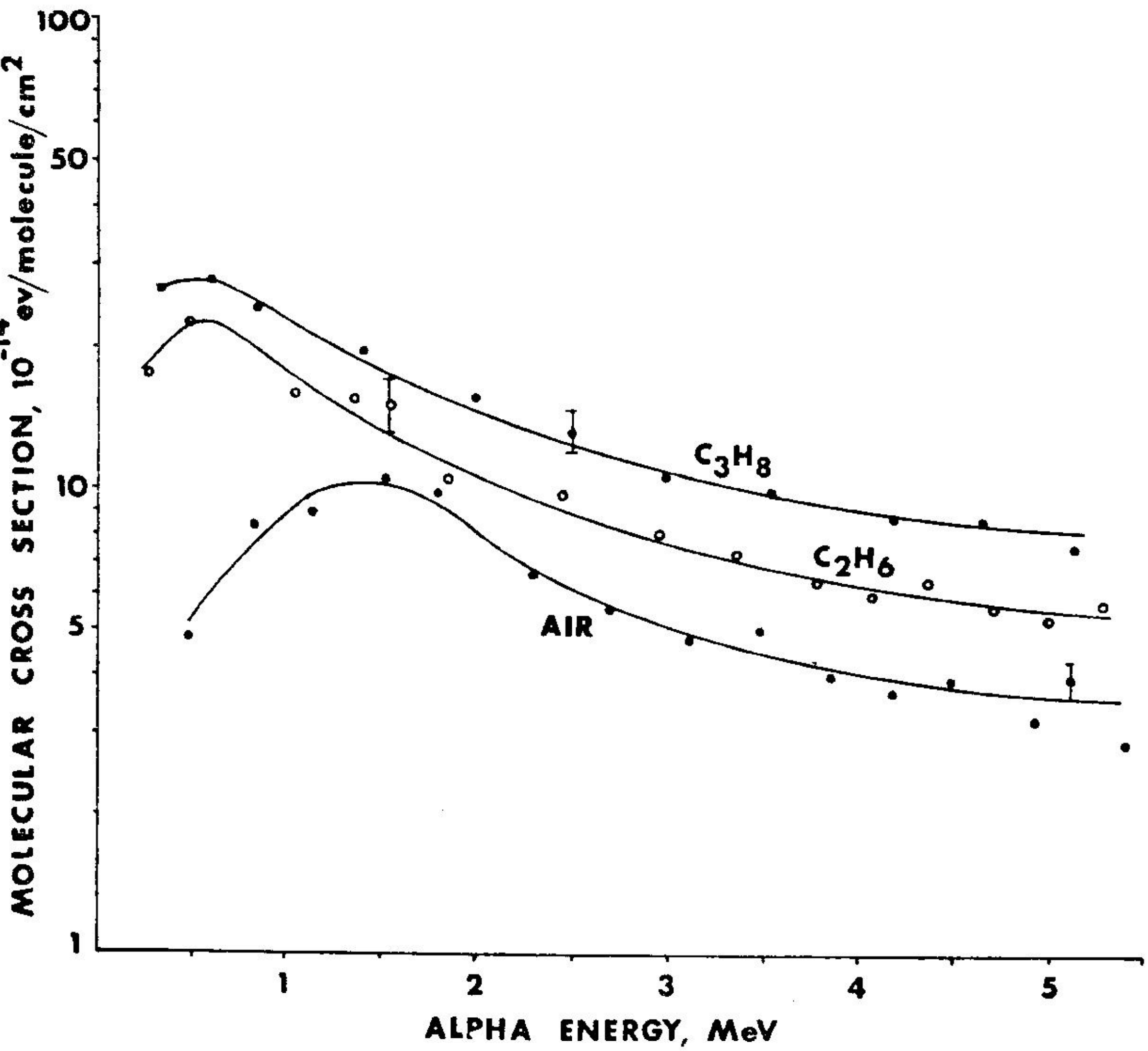

Figure 4.23 : Molecular stopping cross sections of air, C_2H_6 and C_3H_8 for alpha particles.

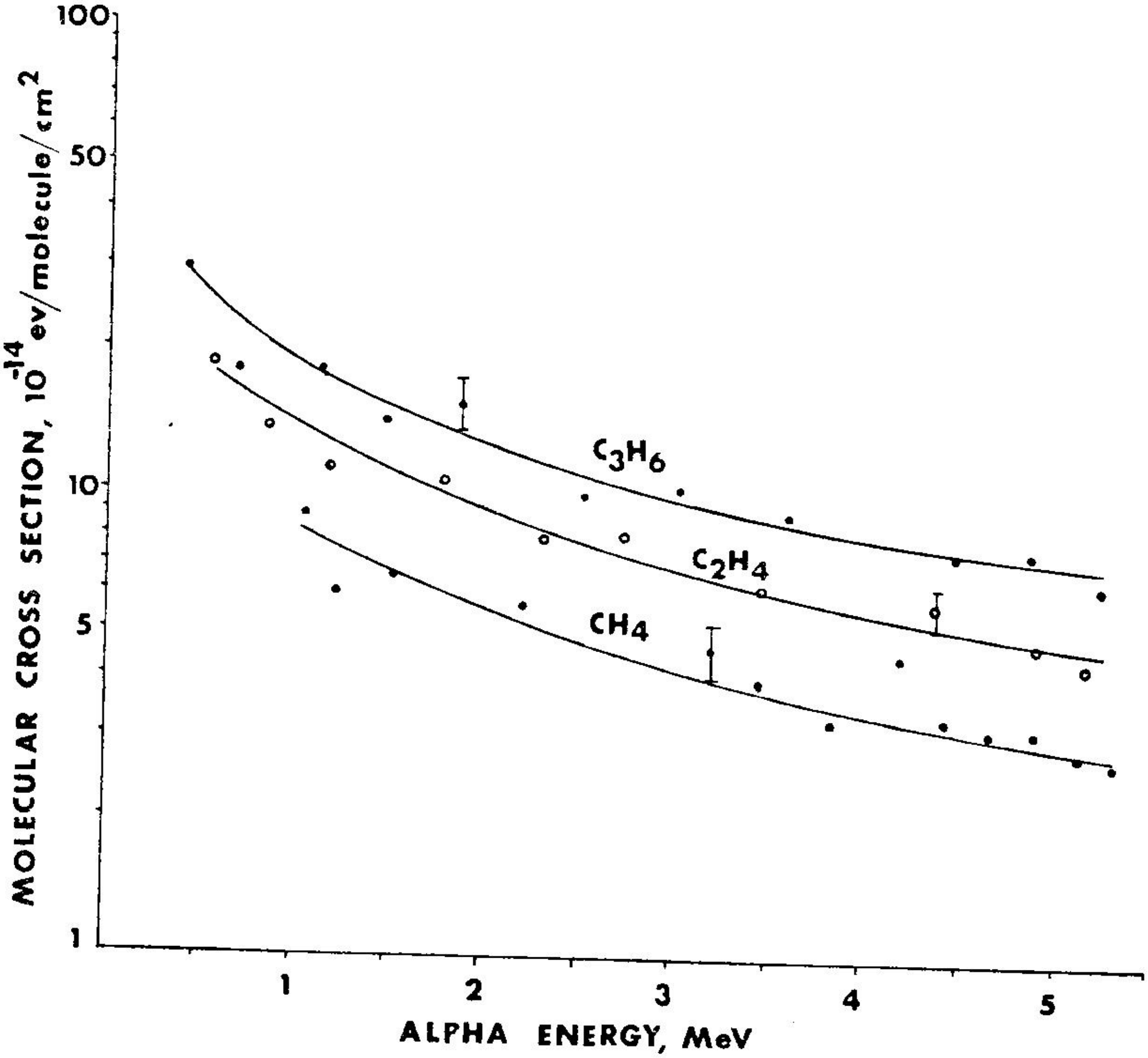

Figure 4.24 : Molecular stopping cross sections of CH_4, C_2H_4 and C_3H_6 for alpha particles.

CHAPTER V

RESULTS AND CONCLUSIONS

The accuracy of the stopping power and molecular cross sections calculated in this investigation depends on the following quantities:

1.- Gas Pressure: The difference between the two columns of the mercury manometer could be read to an accuracy of $\pm$ 0.5 mm of mercury. Thus, the error in P ranged from 0.4 percent for the largest pressure intervals, to 6 percent for the smallest pressure intervals. The pressure intervals ranged from 113 mm of mercury at the highest energies to 8 mm of mercury at the lowest energies.

2.- Gas Temperature: A mean temperature of 24°C was used in calculations and the temperature of the laboratory varied $\pm$ 1°C of this mean. Therefore, the fractional error was approximately 4.0 percent.

3.- Separation Distance of source and detector: The error in the measurement of the separation distance was of the order of 0.8 per cent.

4.- Residual Energy of the alpha particles: This error is the most important in these experiments and the hardest to estimate. However, the estimate of this error seems reasonable from the spread of the experimental data obtained from the energy loss spectra. The uncertainty in estimating the peak channel of the energy spectra was a mayor source of error in determining the average residual energies. At high residual energies, the resolution of the energy analyzing system was very good and the error in locating the peak of the energy spectra was negligible. At low residual energies, straggling of the particles caused the energy spectra to broaden and the peak could not be located with as much accuracy. In this case, the error was estimated to be ± 2 channels, or 0.28 per cent at higher energies and 5.5 per cent at the lower residual energies.

The most probable error of the calculated values based on the experimental data was determined by taking the square root of the sum of the squares of the maximum fractional error in each experiment. At higher residual energies the most probable error (mean standard deviation) found was of the order of 4 - 5 percent and 9 - 10 percent for lower residual energies respectively.

The values proposed by the author on the basis of this investigation for the stopping power of 13 gases are given on figures 4.10 to 4.13 as a function of alpha energies; also, for the molecular cross sections of air and hydrocarbon gases (CH_4, C_2H_4, C_2H_6, C_3H_6, C_3H_8) which are tabulated on Table 4.4. These cross section values were obtained from a smooth curves drawn through the experimental data points and probable errors (figures 4.23 and 4.24) as a function of alpha energy; this is true also for the stopping power and range curves.

The method used in this investigation gives values which are in excellent agreement with those found when the gas pressure within the chamber is constant and the source-detector distance is varied[3] in the energy region where a comparison is possible. Table 5.1 is an example of comparison of molecular cross section calculations given by some authors[8, 15] and this work showing a good correlation within

TABLE 5.1

COMPARISON OF MOLECULAR CROSS SECTION RESULTS WITH DATA FOUND IN LITERATURE

ALPHA PARTICLE ENERGY, MeV	MOLECULAR CROSS SECTION, 10^{-14} ev/molecule/cm^2							
	A I R [8]		METHANE (CH_4) [8]		ETHYLENE (C_2H_4) [15]		PROPANE (C_3H_8) [15]	
	Kerr et al.	This work	Kerr et al.	This work	Walsh	This work	Walsh	This work
0.6	9.5	6.2	12.0	-	16.6	17.5	27.6	27.6
0.8	9.9	7.7	10.8	10.0	14.6	15.5	23.9	26.0
1.0	9.4	9.2	9.5	8.5	13.4	13.8	21.9	24.0
1.2	8.6	9.9	8.5	7.5	12.5	12.5	20.3	22.6
1.4	8.1	10.0	7.7	6.8	11.2	11.3	18.2	19.3
1.6	7.6	9.5	7.1	6.3	10.2	10.4	16.6	17.4
1.8	7.2	8.7	6.6	5.9	9.8	9.6	16.1	16.0
2.0	6.8	8.0	6.1	5.5	9.3	8.9	14.6	14.6
2.5	6.0	6.2	5.3	4.9	8.1	7.7	13.1	13.3
3.0	5.3	5.1	4.6	4.3	7.2	6.7	11.7	10.9
3.5	4.7	4.4	4.1	3.9	6.3	6.1	10.2	9.7

CONT. TABLE 5.1

ALPHA PARTICLE ENERGY, MeV	MOLECULAR CROSS SECTION, 10^{-14} ev/molecule/cm^2 AIR		METHANE (CH_4)		ETHYLENE (C_2H_4)		PROPANE (C_3H_8)	
	Kerr et al.[8]	This work	Kerr et al.[8]	This work	Walsh[15]	This work	Walsh[15]	This work
4.0	4.3	3.9	3.7	3.5	5.5	5.6	9.8	9.1
4.5	3.9	3.7	3.4	3.2	5.1	5.1	8.9	8.4
5.0	3.6	3.5	3.1	2.9	4.7	4.8	7.3	8.0

the 0.6 - 5.0 Mev alpha energy region for some hydrocarbon gases and air. This work could be extended indefinitely for additional molecular cross section calculations using the information on inorganic gases (A_2, N_2, O_2, CO_2, N_2O, etc) given in this work or including as many inorganic and organic research and industrial gases as desired. In the same way, comparisons with theoretical calculations using the Bethe's equation (Eq. 3.17) agree when the residual alpha energy is higher than 1 Mev. (See Figure 5.1).

In the radiolysis of a gaseous system it is possible to measure the number of ion pairs formed by absorption of radiation. The yield of a given reaction can therefore be expressed in terms of the number of molecules changed per ion pair formed. The ratio M/N_i is commonly referred to as the ion pair yield, where M is the number of molecules changed per ion pair and N_i is the number of ion pairs formed. M may designate a species of a given kind disappearing or being produced, and in a mixture of gases, N_i may be expressed either as the total number of ions or as the number of ions of a given kind. The latter calculation is based on a knowledge of stopping powers and the energy required to produce an ion pair in the individual gases. Related research could be developed simultaneously like gas radiolysis, determination of chemical reaction mechanisms, ion yield measurements, etc, using the values given in this work for inorganic and hydrocarbon gases.

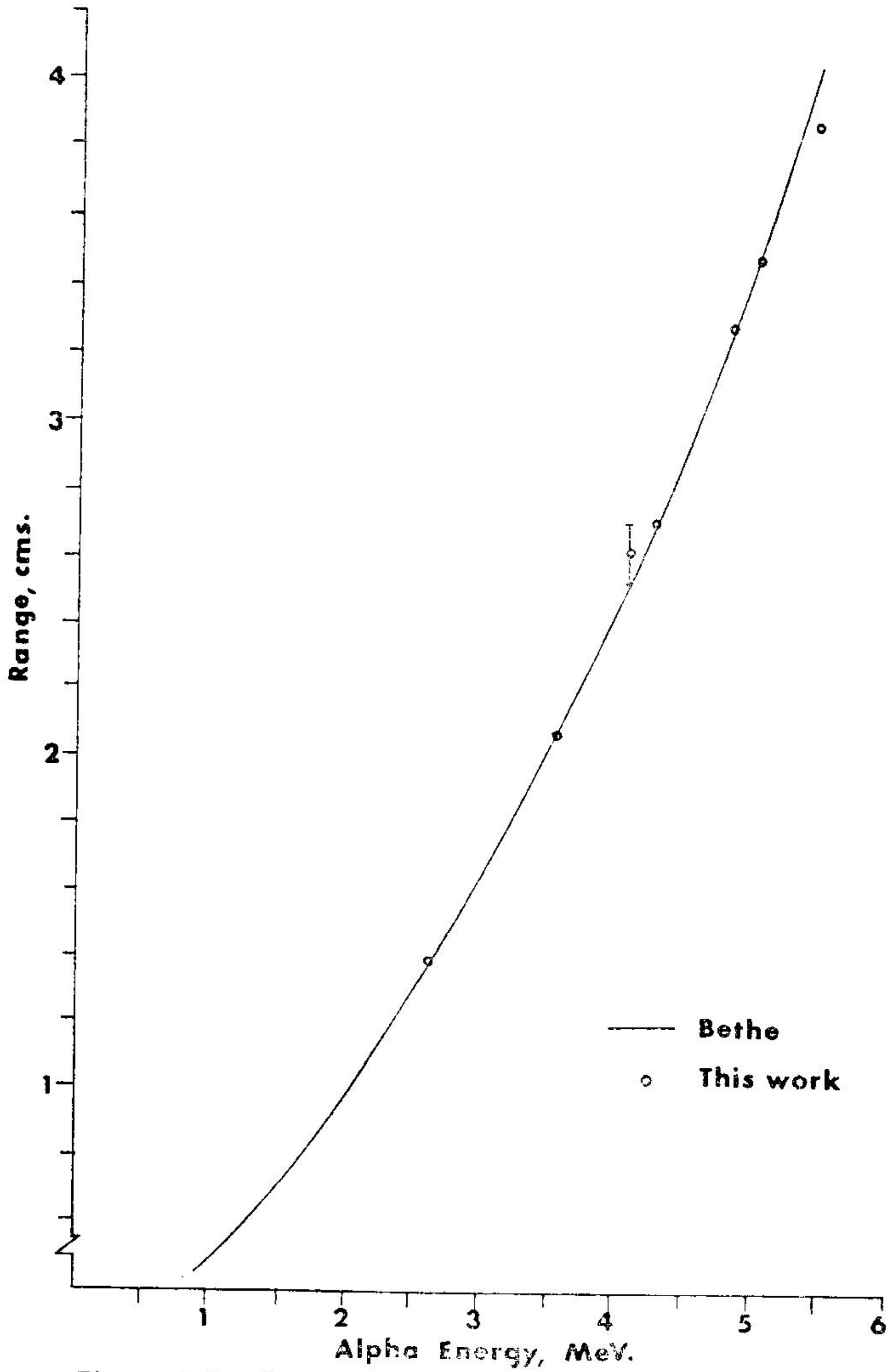

Figure 5.1 : Range-energy relation of slow alpha particles in air at standard conditions.

BIBLIOGRAPHY

1.- ALLISON, S.K. and WARSHAW, S.D.: The Stopping Cross Sections for Protons, 0.1 to 6.0 Mev; Rev. Mod. Phys. 25, 779 (1953).

2.- BENT, H.A.: Chemical Structures of Inorganic Gases; J. Chem. Educ. 37, 616 (1960).

3.- BETHE, H.A.: The Range-Energy Relations for Slow Alpha Particles and Protons in Air; Rev. Mod. Phys. 22, 213 (1950).

4.- BOURLAND, P.D., CHU, W.K. and POWERS, D.: Stopping Cross Sections of Gases for Alpha Particles from 0.3 to 2.0 Mev; Phys. Rev. B3, 3625 (1971).

5.- COLARD, J. and GAL, J.: Silicon Surface-Barrier Type Semiconductor Detectors; Nucl. Instrum. Meth. 16, 195 (1962)

6.- DEARNALEY, G.: Semiconductor Nuclear Particle Detectors; National Academy of Sciences - National Research Council Publication 871 (Edited by J.W.T. Dabbs and F.J. Walter), pp.49 (1961).

7.- JESSE, W.P. and SADAUSKIS, J.: The Range-Energy Curves for Alpha Particles and Protons; Phys. Rev. 78, 1 (1950).

8.- KERR, G.D., HAIRR, L.M., UNDERWOOD, N. and WALTNER, A.W.: Molecular Stopping Cross Sections of Air, N_2, Kr, CO_2 and CH_4 for Alpha Particles; Health Phys. 12, 1475 (1966).

9.- LIND, S.C.: Radiation Chemistry of Gases; Reinhold Publishing Corp. New York, N.Y., pp. 123 (1961).

10.- ORVILLE, W.J. and THOMAS, J.: Mol. Spectry. 3, 588 (1958).

11.- PALMER, R.B.J.: The Stopping Power of Hydrogen and Hydrocarbon Vapours for Alpha Particles over the Energy Range 1 - 8 Mev; Proc. Phys. Soc. 87, 681 (1966).

12.- PAULING, L.: The Chemical Bond; Cornell University Press, Ithaca N.Y. pp. 58 (1967).

13.- ROTONDI, E.: Energy Loss of Alpha Particles in Tissue; Radiation Res. 33, 1 (1968).

14.- SEGRE, E. (Editor): Experimental Nuclear Physics; vol.1, part II, pp. 166 Wileg (1953).

15.- WALAH, P.J.: Energy Loss of Alpha Particles, Protons and Electrons in Matter; Ph. D. Thesis, University of North Carolina, Chapel Hill, N.C. (1968).

16.- WEAST, R.C. (Editor): Handbook of Chemistry and Physics; Chemical Rubber Co., Cleveland (1966).

APENDIX

TABLE A.1

INSTRUMENTATION EQUIPMENT SETTINGS FOR EXPERIMENTS

1.- DETECTOR BIAS SUPPLY

Ortec Model 428

Gate A: 50 volts.

2.- TIMER

Ortec Model 719

Preset time : 400 seconds.

3.- AMPLIFIER & PULSE HEIGHT ANALYZER

Ortec Model 486

Coarse gain: 16 volts

Fine gain: 6.5 volts

Window: 10 volts

Lower level: 0.52 volts

Other settings as per operating instructions.

4.- SCALER

Ortec Model 484

Threshold: 0.4

Other settings as per operating instructions.

5.- ANALOG TO DIGITAL CONVERTER

Nuclear Data

Zero Fine: 0.40 volts

Zero Coarse: 10.0 volts.

CONT. TABLE A.1

Conversion Gain: 1024 ch.

Upper Level Discriminator: 10 volts.

Lower Level Discriminator: 0.49 volts

Other settings as per operating instructions.

6.- MASTER CONTROL

Nuclear Data

Preset time: 400 seconds.

Other settings as per operating instructions.

7.- READ-IN/OUT DISPLAY

Nuclear Data

Settings as per operating instructions.

TABLE A.2

RANGE AND ENERGY LOSS EXPERIMENTAL DATA FOR 5.477-MEV Am^{241} ALPHA PARTICLES IN AIR

CHAMBER PRESSURE, cms of Hg	TOTAL COUNTS	RATIO	X_{stp}, cms	CHANNEL NUMBER	EQUIVALENT ENERGY, MeV
0.1	1726	1.011	0.007	708	5.47
4.1	1678	0.983	0.291	678	5.27
8.5	1707	1.000	0.604	639	4.96
10.5	1643	0.962	0.746	622	4.85
12.9	1658	0.971	0.916	595	4.60
16.9	1603	0.939	1.200	557	4.32
21.9	1656	0.970	1.556	517	4.00
26.1	1636	0.958	1.854	475	3.70
30.7	1644	0.963	2.181	423	3.29
35.3	1623	0.950	2.508	373	2.90
39.3	1621	0.949	2.792	323	2.50
42.7	1627	0.953	3.033	272	2.10
46.7	1629	0.954	3.318	127	1.00
51.3	1549	0.907	3.644	113	0.87
52.3	1299	0.761	3.716	103	0.80
53.0	1085	0.635	3.765	92	0.71
54.0	417	0.244	3.836	67	0.52
54.8	36	0.002	3.893	58	0.45

TABLE A.3

RANGE AND ENERGY LOSS EXPERIMENTAL DATA FOR 5.477-MEV Am^{241} ALPHA PARTICLES IN CH_4

CHAMBER PRESSURE, cms of Hg	TOTAL COUNTS	RATIO	X_{stp}, cms	CHANNEL NUMBER	EQUIVALENT ENERGY, MeV
0.4	1716	1.000	0.028	699	5.43
5.0	1638	0.954	0.355	671	5.21
9.0	1671	0.973	0.639	645	5.01
13.1	1694	0.987	0.930	615	4.78
17.4	1669	0.972	1.236	585	4.54
21.2	1639	0.955	1.506	556	4.32
25.4	1638	0.954	1.804	522	4.05
32.4	1603	0.934	2.302	462	3.59
36.2	1686	0.982	2.572	428	3.32
41.4	1580	0.920	2.941	372	2.89
46.9	1605	0.935	3.332	315	2.45
52.1	747	0.435	3.701	249	1.93
53.7	71	0.040	3.815	210	1.63
54.1	23	0.012	3.843	-	-
56.1	8	0.004	3.986	179	1.39
59.5	1	0.000	4.227	131	1.02
60.1	1	0.000	4.270	84	0.65

TABLE A.4

RANGE AND ENERGY LOSS EXPERIMENTAL DATA FOR 5.477-MEV Am^{241} ALPHA PARTICLES IN C_2H_6

CHAMBER PRESSURE, cms of Hg	TOTAL COUNTS	RATIO	X_{stp}, cms	CHANNEL NUMBER	EQUIVALENT ENERGY, MeV
0.8	1668	0.989	0.056	698	5.42
3.6	1602	0.950	0.255	662	5.14
7.0	1636	0.970	0.497	621	4.82
9.7	1685	1.000	0.688	586	4.55
12.7	1583	0.939	0.901	542	4.21
15.4	1584	0.940	1.093	505	3.92
18.6	1608	0.954	1.320	458	3.55
21.6	1518	0.936	1.533	408	3.17
24.6	1612	0.956	1.746	353	2.74
28.0	1646	0.976	1.988	277	2.15
31.6	1547	0.918	2.243	191	1.48
34.8	688	0.408	2.470	73	0.56
35.4	58	0.034	2.513	43	0.33
36.0	0	0.000	2.556	25	0.19

TABLE A.5

RANGE AND ENERGY LOSS EXPERIMENTAL DATA FOR 5.477-MEV Am^{241} ALPHA PARTICLES IN C_3H_8

CHAMBER PRESSURE, cms of Hg	TOTAL COUNTS	RATIO	X_{stp}, cms	CHANNEL NUMBER	EQUIVALENT ENERGY, MeV
1.0	1613	0.959	0.071	693	5.38
5.0	1681	1.000	0.355	623	4.84
7.6	1623	0.965	0.540	573	4.45
11.1	1643	0.977	0.788	503	3.90
15.1	1596	0.949	1.072	413	3.20
17.5	1604	0.954	1.243	354	2.75
19.9	1565	0.930	1.413	284	2.20
21.7	1552	0.923	1.541	221	1.71
23.5	1487	0.884	1.669	140	1.08
24.1	1430	0.850	1.712	123	0.95
24.9	546	0.324	1.769	92	0.71
25.5	202	0.120	1.811	65	0.50
26.3	1	0.000	1.850	15	0.11

TABLE A.6

RANGE AND ENERGY LOSS EXPERIMENTAL DATA FOR 5.477-MEV Am^{241} ALPHA PARTICLES IN C_2H_4

CHAMBER PRESSURE, cms of Hg	TOTAL COUNTS	RATIO	X_{stp}, cms	CHANNEL NUMBER	EQUIVALENT ENERGY, MeV
0.7	1699	0.990	0.049	702	5.45
2.9	1715	1.000	0.206	679	5.27
5.9	1706	0.994	0.419	649	5.04
8.9	1681	0.980	0.632	616	4.78
11.9	1682	0.980	0.845	582	4.52
14.9	1604	0.935	1.058	543	4.21
17.0	1681	0.980	1.207	504	3.98
21.0	1641	0.956	1.492	466	3.62
24.0	1680	0.980	1.705	423	3.28
27.0	1648	0.960	1.918	380	2.95
30.0	1561	0.910	2.131	325	2.52
33.2	1680	0.980	2.358	267	2.07
36.0	1503	0.876	2.557	206	1.60
37.0	1545	0.900	2.628	174	1.35
38.7	1504	0.876	2.749	130	1.01
40.1	1254	0.731	2.849	88	0.68
40.9	200	0.116	2.906	54	0.41
41.3	22	0.012	2.934	52	0.40
41.7	1	0.0005	2.962	30	0.23

TABLE A.7

RANGE AND ENERGY LOSS EXPERIMENTAL DATA FOR 5.477-MEV Am^{241} ALPHA PARTICLES IN C_3H_6

CHAMBER PRESSURE, cms of Hg	TOTAL COUNTS	RATIO	X_{stp}, cms	CHANNEL NUMBER	EQUIVALENT ENERGY, MeV
0.8	1715	1.000	0.056	696	5.40
3.8	1619	0.944	0.270	653	5.07
6.8	1645	0.959	0.483	601	4.67
9.8	1690	0.985	0.696	550	4.27
12.8	1675	0.976	0.909	494	3.83
15.9	1683	0.981	1.129	431	3.34
18.9	1651	0.962	1.343	360	2.79
21.9	1618	0.943	1.555	294	2.28
25.0	1600	0.932	1.776	186	1.44
27.0	1347	0.785	1.918	105	0.81
27.8	355	0.207	1.975	72	0.55
28.4	4	0.002	2.017	32	0.24
28.8	0	0.000	2.046	20	0.15

TABLE A.8

RANGE AND ENERGY LOSS EXPERIMENTAL DATA FOR 5.477-MEV Am^{241} ALPHA PARTICLES IN N_2O

CHAMBER PRESSURE, cms of Hg	TOTAL COUNTS	RATIO	X_{stp}, cms	CHANNEL NUMBER	EQUIVALENT ENERGY, MeV
0.7	1671	0.991	0.050	699	5.43
3.1	1706	1.012	0.220	667	5.18
6.7	1670	0.991	0.476	622	4.83
10.1	1674	0.993	0.717	577	4.48
13.3	1653	0.981	0.945	530	4.11
16.9	1685	1.000	1.200	475	3.69
20.8	1619	0.960	1.477	417	3.24
25.8	1565	0.930	1.833	344	2.67
27.1	1592	0.945	1.925	271	2.10
32.1	1532	0.910	2.280	169	1.31
34.2	1399	0.830	2.430	109	0.84
34.8	1192	0.707	2.472	92	0.71
35.7	153	0.090	2.536	67	0.52
36.1	10	0.005	2.565	49	0.38
36.9	2	0.000	2.621	26	0.20

TABLE A.9

RANGE AND ENERGY LOSS EXPERIMENTAL DATA FOR 5.477-MEV Am^{241} ALPHA PARTICLES IN O_2

CHAMBER PRESSURE, cms of Hg	TOTAL COUNTS	RATIO	X_{stp}, cms	CHANNEL NUMBER	EQUIVALENT ENERGY, MeV
0.8	1701	1.007	0.056	703	5.46
2.8	1682	0.995	0.199	688	5.34
6.6	1617	0.957	0.469	652	5.06
10.2	1621	0.959	0.724	618	4.80
15.0	1602	0.948	1.065	572	4.44
19.0	1689	1.000	1.350	533	4.14
23.0	1635	0.968	1.634	495	3.84
27.0	1643	0.972	1.918	448	3.48
31.0	1623	0.960	2.202	393	3.05
35.0	1639	0.970	2.486	348	2.70
39.8	1514	0.896	2.827	279	2.16
42.9	1522	0.901	3.048	232	1.80
47.5	1528	0.904	3.374	138	1.07
50.0	1454	0.860	3.550	112	0.87
50.5	466	0.275	3.588	73	0.56
51.0	120	0.071	3.621	54	0.42
52.1	1	0.000	3.701	34	0.26

TABLE A.10

RANGE AND ENERGY LOSS EXPERIMENTAL DATA FOR 5.477-MEV Am^{241} ALPHA PARTICLES IN N_2

CHAMBER PRESSURE, cms of Hg	TOTAL COUNTS	RATIO	X_{stp}, cms	CHANNEL NUMBER	EQUIVALENT ENERGY, MeV
0.8	1697	1.000	0.056	705	5.47
4.8	1758	1.035	0.341	672	5.22
8.8	1688	0.994	0.625	637	4.94
14.8	1652	0.973	1.051	590	4.58
20.8	1588	0.935	1.477	534	4.14
24.8	1624	0.956	1.762	496	3.85
28.8	1567	0.923	2.046	458	3.55
32.8	1651	0.973	2.330	412	3.20
37.4	1607	0.947	2.657	361	2.80
41.0	1636	0.964	2.913	314	2.43
45.0	1614	0.951	3.197	260	2.02
48.8	1560	0.919	3.467	203	1.57
50.6	1513	0.891	3.595	172	1.33
52.0	1573	0.926	3.694	138	1.07
52.8	1431	0.843	3.751	126	0.97
53.9	1339	0.789	3.829	98	0.76
54.7	805	0.474	3.886	82	0.63
55.3	389	0.217	3.929	72	0.55
55.8	78	0.010	3.964	56	0.43
56.2	5	0.001	3.993	47	0.36

TABLE A.11

RANGE AND ENERGY LOSS EXPERIMENTAL DATA FOR 5.477-MEV Am^{241} ALPHA PARTICLES IN A

CHAMBER PRESSURE, cms of Hg	TOTAL COUNTS	RATIO	X_{stp}, cms	CHANNEL NUMBER	EQUIVALENT ENERGY, MeV
2.4	1676	0.988	0.170	690	5.36
6.4	1731	1.021	0.454	659	5.12
10.1	1607	0.948	0.717	620	4.87
14.1	1625	0.958	1.001	598	4.64
18.9	1628	0.960	1.342	559	4.34
22.7	1666	0.982	1.612	523	4.06
26.9	1686	0.994	1.911	482	3.74
31.3	1695	1.000	2.223	440	3.41
34.9	1574	0.928	2.479	402	3.12
40.3	1599	0.943	2.863	339	2.63
44.8	1515	0.893	3.183	284	2.20
48.3	1450	0.855	3.431	241	1.87
52.1	1465	0.864	3.701	182	1.41
55.5	1438	0.848	3.943	125	0.97
56.3	1356	0.800	4.000	102	0.79
58.1	517	0.305	4.128	70	0.54
59.5	52	0.030	4.227	52	0.40
59.9	0	0.000	4.255	27	0.20

TABLE A.12

RANGE AND ENERGY LOSS EXPERIMENTAL DATA FOR 5.477-MEV Am^{241} ALPHA PARTICLES IN CO_2

CHAMBER PRESSURE, cms of Hg	TOTAL COUNTS	RATIO	X_{stp}, cms	CHANNEL NUMBER	EQUIVALENT ENERGY, MeV
0.4	1705	0.993	0.028	700	5.43
1.4	1656	0.970	0.099	687	5.33
3.2	1707	1.000	0.227	669	5.18
5.4	1674	0.980	0.383	640	4.97
7.3	1698	0.994	0.518	615	4.77
9.5	1663	0.974	0.675	588	4.56
12.5	1659	0.971	0.888	544	4.22
15.1	1638	0.959	1.072	505	3.92
18.6	1659	0.971	1.321	457	3.55
20.6	1595	0.934	1.463	423	3.28
23.2	1549	0.907	1.648	380	2.95
24.6	1583	0.927	1.748	346	2.68
27.0	1569	0.919	1.918	304	2.34
29.8	1632	0.923	2.117	235	1.80
33.0	1524	0.892	2.344	151	1.16
35.2	966	0.566	2.499	82	0.63
36.2	44	0.025	2.570	56	0.43
37.2	0	0.000	2.641	24	0.18

TABLE A. 13

RANGE AND ENERGY LOSS EXPERIMENTAL DATA FOR 5.477-MEV Am^{241} ALPHA PARTICLES IN Kr

CHAMBER PRESSURE, cms of Hg	TOTAL COUNTS	RATIO	X_{stp}, cms	CHANNEL NUMBER	EQUIVALENT ENERGY, MeV
0.4	1657	0.982	0.028	704	5.47
4.4	1687	1.000	0.312	654	5.08
9.1	1662	0.985	0.646	596	4.63
13.9	1662	0.985	0.987	535	4.15
18.9	1567	0.928	1.342	473	3.67
23.5	1484	0.880	1.669	405	3.14
27.2	1404	0.832	1.932	353	2.74
31.0	1347	0.798	2.202	284	2.20
33.0	234	0.138	2.344	238	1.84
34.0	29	0.017	2.415	229	1.77
35.0	8	0.004	2.486	206	1.60
35.9	1	0.000	2.550	185	1.43
36.7	1	0.000	2.607	168	1.30
38.3	0	0.000	2.721	135	1.04
40.1	0	0.000	2.842	89	0.63

TABLE A.14

RANGE AND ENERGY LOSS EXPERIMENTAL DATA FOR 5.477-MEV Am^{241} ALPHA PARTICLES IN FREON 14

CHAMBER PRESSURE, cms of Hg	TOTAL COUNTS	RATIO	X_{stp}, cms	CHANNEL NUMBER	EQUIVALENT ENERGY, MeV
0.8	1679	0.997	0.056	693	5.38
3.8	1683	1.000	0.270	624	4.85
6.8	1645	0.977	0.483	550	4.27
10.1	1656	0.984	0.717	466	3.62
12.9	1630	0.968	0.916	381	2.96
15.9	1625	0.965	1.129	280	2.17
18.7	1544	0.917	1.328	150	1.16
19.8	1203	0.714	1.406	90	0.70
20.4	112	0.066	1.449	62	0.48
21.0	2	0.000	1.501	34	0.26